

# 1 **Spatiotemporal control for integrated catalysis**

2 Shijie Deng,<sup>1,#</sup> Brandon J. Jolly,<sup>1,#</sup> James R. Wilkes,<sup>2</sup> Yu Mu,<sup>2</sup> Jeffery A. Byers,<sup>2</sup> Loi H. Do,<sup>3</sup> Alexander J. M.  
3 Miller,<sup>4</sup> Dunwei Wang,<sup>2</sup> Chong Liu,<sup>1</sup> and Paula L. Diaconescu<sup>1\*</sup>

4 <sup>1</sup>Department of Chemistry and Biochemistry, University of California, Los Angeles, 607 Charles E. Young  
5 Drive East, Los Angeles, California 90095, United States

6 <sup>2</sup>Department of Chemistry, Eugene F. Merkert Chemistry Center, Boston College, 2609 Beacon Street,  
7 Chestnut Hill, Massachusetts 02467, United States

8 <sup>3</sup>Department of Chemistry, University of Houston, 4800 Calhoun Road, Houston, Texas 77004, United  
9 States

10 <sup>4</sup>Department of Chemistry, University of North Carolina at Chapel Hill, Chapel Hill, North Carolina 27599-  
11 3290, United States

12 <sup>#</sup>These authors contributed equally.

13 <sup>\*</sup>Corresponding author: pld@chem.ucla.edu

## 14 **Abstract**

15 Integrated catalysis is an emerging methodology that can streamline the multistep synthesis of  
16 complicated products in a single reaction vessel, achieving a high degree of control and reducing the waste  
17 and cost of an overall chemical process. Integrated catalysis can be defined by the use of spatial and  
18 temporal control to couple different catalytic cycles in one pot. This primer discusses commonly employed  
19 approaches and their underlying mechanisms, and elaborates on how the integration of spatially and  
20 temporally controlled catalysis in one pot can deliver the synthesis of complex products with high  
21 efficiency. We highlight recent advances, analyze current applications and limitations, and provide an  
22 outlook for the future development of integrated catalysis.

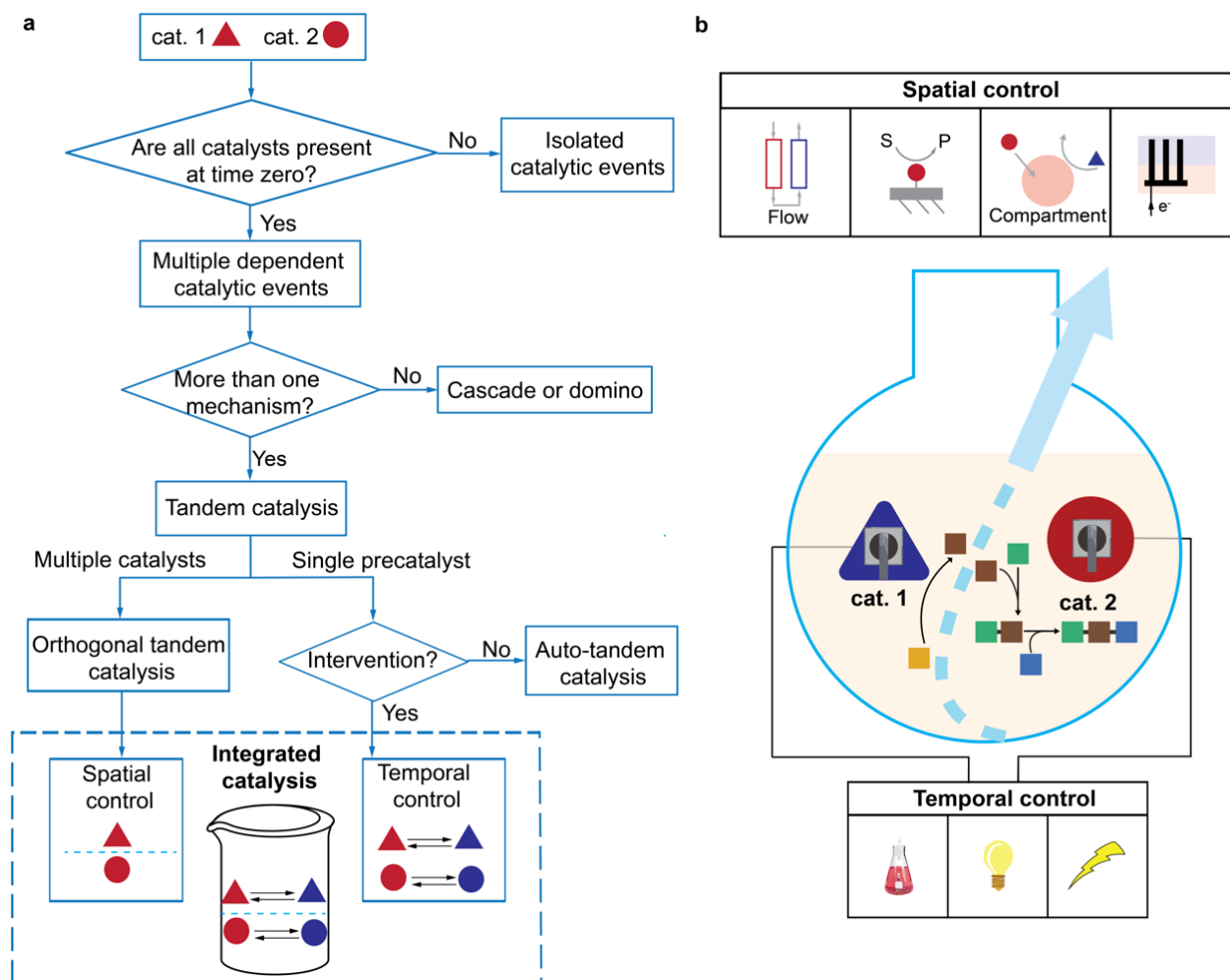
## 23 [H1] Introduction

24 Chemical synthesis plays a crucial role in modern technology and everyday life. From plastics to  
25 pharmaceuticals, virtually every facet of society is impacted by our ability to construct small molecules  
26 and macromolecules. A major focus in chemical research is the development of efficient methods for the  
27 production of synthetic chemicals. In 2017, the chemical industry was responsible for 10% of the total  
28 annual global energy consumption (and 28% of industrial energy consumption).<sup>1,2</sup> Thus, alternative  
29 approaches to chemical synthesis that minimize energy consumption and increase efficiency are needed.

30 The majority of commodity chemicals, pharmaceuticals and consumer materials are prepared in multistep  
31 syntheses that require catalysts to achieve high yields with selectivity toward the desired products.<sup>3</sup> A  
32 drawback of such methods is that they require time, energy, and exhaustive effort between reaction steps  
33 to separate and purify stable reaction intermediates. Alternative methods that enable multistep  
34 sequences would remove the need to isolate such species. A particularly attractive approach for chemical  
35 synthesis is integrated catalysis, in which multiple catalysts are carefully controlled and positioned to  
36 allow efficient multistep reaction sequences, funneling products generated by one catalyst to the next.

37 A combination of catalytic processes, either involving one catalyst or multiple catalysts with orthogonal  
38 reactivity, (FIG. 1a)<sup>4</sup> may be classified as a **cascade or domino process [G]** if only one linear reaction  
39 sequence occurs. If multiple reactions are proceeding simultaneously, then it is considered a **tandem**  
40 **process [G]**. Examples of integrated catalysis are often special cases of tandem catalysis, in which multiple  
41 catalysts operate through orthogonal mechanisms synergistically or can be switched on/off using external  
42 triggers. The recent literature has many excellent examples of cascade or tandem processes,<sup>4-20</sup> but  
43 integrated processes are rarely reported. Multiple catalytic processes operating together could be solely  
44 chemo- or bio- based, or a combination of the two. In this primer, we will focus on chemocatalytic  
45 systems.

46 Integrated reactions hold promise to be more efficient than an iterative process; combining spatial and  
47 temporal control avoids the need for separation and purification of intermediate steps. Furthermore,  
48 combining spatial and temporal control may also lead to the development of new chemistry and novel  
49 products. For example, a hypothetical integrated catalytic system (FIG. 1b) with spatiotemporal control  
50 can allow the efficient conversion of a starting material (gold square) to an intermediate (brown square).  
51 This intermediate can diffuse to another part of the reactor where a second catalyst, spatially separated  
52 so as not to interact with the first catalyst, reacts with and couples the intermediate with a second  
53 reactant (green square). The second catalyst may also be temporally switched to a state where it is now  
54 active for the incorporation of a third reactant (blue square). This approach could be a general strategy to  
55 synthesize complex structures that are not accessible using conventional methods, as such methods do  
56 not typically consider spatial and temporal control.



57

58 **Fig. 1 | Concept of integrated catalysis.** a | A flowchart guide to nomenclature of different multistep one-pot catalytic  
 59 processes. b | Illustration of integrated catalysis. In a hypothetical integrated catalytic system with spatiotemporal  
 60 control, the starting material (gold square) is efficiently converted to an intermediate (brown square). This  
 61 intermediate could then react with another catalyst that would combine the synthesized intermediate with another  
 62 reactant (green square). The second catalyst can also be switched on to incorporate a third reactant (blue square).  
 63 This approach can be a general strategy for synthesizing complex structures that are not available by conventional  
 64 methods. Temporal control methods include external stimuli, e.g., chemical reagents, light, electron transfer, etc.,  
 65 whereas spatial control can be achieved by using flow chemistry, immobilization, compartmentalization, and  
 66 microscopic concentration gradients.

67

68 To enable multiple catalysts to operate concurrently, issues relating to compatibility must be overcome.  
 69 For example, potentially problematic catalyst-catalyst, catalyst-reactant, and catalyst-product  
 70 interactions need to be addressed. To reconcile potential incompatibility, spatial and/or temporal control  
 71 are required to manipulate where and when certain processes occur. Spatial control may be employed to  
 72 localize and separate catalysts or entire catalytic systems from each other. This may be achieved in a  
 73 number of approaches (vide infra), namely **compartmentalization** [G],<sup>8,21-27</sup> immobilization onto a

74 surface,<sup>28-35</sup> or by taking advantage of microscopic concentration gradients.<sup>18,20,36,37</sup> By preventing  
75 incompatible species from coming into contact with each other, efficient integrated processes may be  
76 promoted. In addition to spatial control, introducing temporal control can also alleviate compatibility  
77 concerns. If two processes compete with or hinder each other's activity, deactivating one while the other  
78 is active can help avoid incompatibility. Temporal control may be achieved using a variety of external  
79 stimuli<sup>38-41</sup> to switch between different states of a catalyst that have **orthogonal reactivity [G]** toward  
80 certain substrates.

81 In this primer, approaches to achieve spatial and temporal control in catalysis to achieve integrated  
82 catalysis are discussed. Seminal studies illustrating spatiotemporal control of catalysts will be presented  
83 to showcase their impact on some of the most challenging problems in catalysis. The development of a  
84 toolbox for integrated catalysis is also discussed, followed by limitations and suggested optimizations for  
85 this nascent field of research. Lastly, the direction in which integrated catalysis is likely to make progress  
86 in the next 5-10 years is discussed.

87

## 88 **[H1] Experimentation**

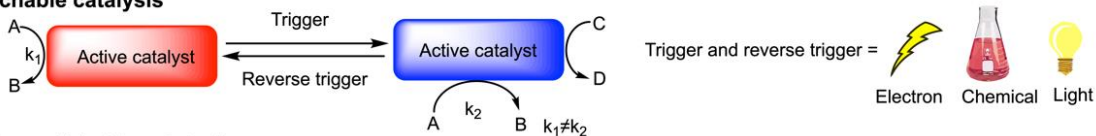
89 This section outlines considerations for the temporal and spatial control of a number of catalytic systems.  
90 By the use of examples, reaction processes and mechanisms are discussed, as well as considerations for  
91 each catalytic system. The typical setup for catalytic systems and design considerations for such systems  
92 are described.

## 93 **[H2] Temporal control**

94 In nature, living organisms have the ability to respond to environmental factors, causing them to behave  
95 differently or take on different forms. At the microscopic level, external stimuli regulate feedback loops  
96 and modulate enzymatic reactions within cells to effect biological changes. Taking inspiration from nature,  
97 scientists have been working on artificial catalytic systems that could be tuned reversibly by external  
98 stimuli. In such switchable systems, a catalyst could be toggled on/off or may oscillate between different  
99 catalytic states to achieve orthogonal reactivity. Depending on the application and reaction conditions,  
100 different external stimuli can be used to implement a switchable behavior. In this section, redox, chemo-,  
101 and photo-switching will be discussed, with a focus on the switching mechanisms and general catalyst  
102 design concepts. Several comprehensive reviews have been published on temporally switchable  
103 catalysis.<sup>38,40-43</sup>

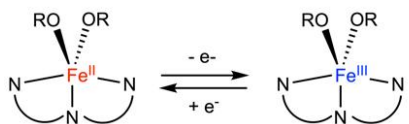
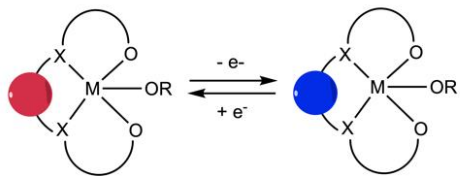
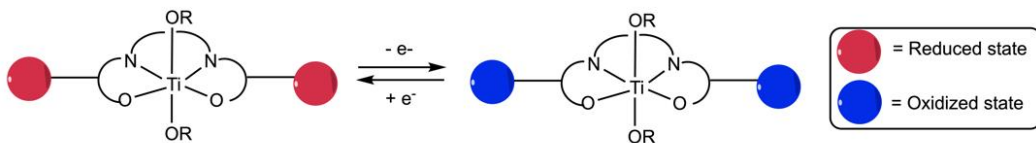
104

### a Switchable catalysis

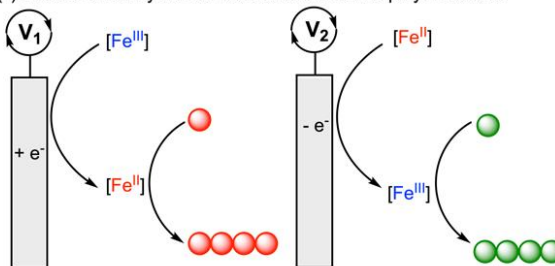


### b Redox switchable catalysis

(i) Redox switchable metal catalyst

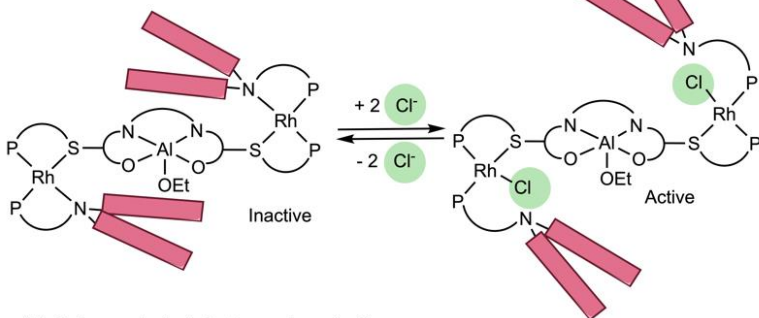


(ii) Electrochemically controlled redox switchable polymerization

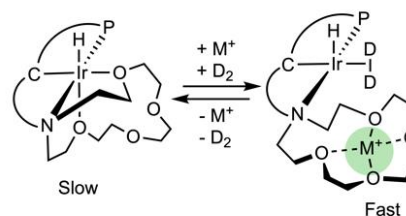


### c Chemoswitchable catalysis

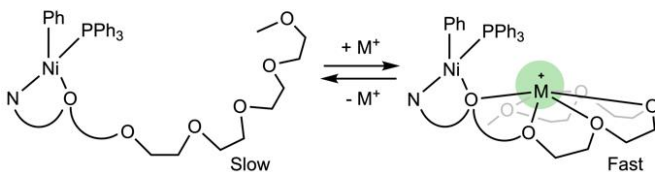
(i) Allosteric controlled lactone polymerization



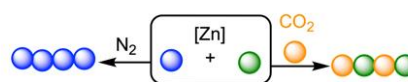
(ii) Cation controlled hydrogen activation



(iii) Cation controlled ethylene polymerization

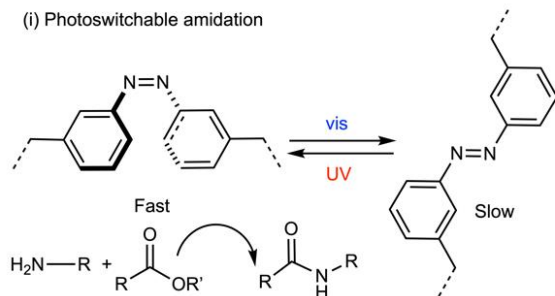


(iv) CO<sub>2</sub> controlled polymerization

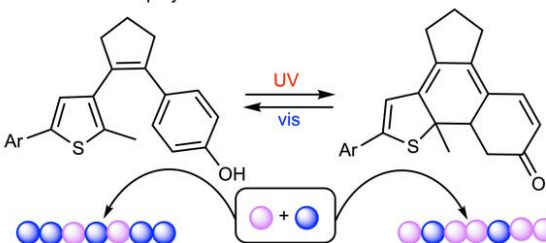


### d Photoswitchable catalysis

(i) Photoswitchable amidation



(ii) Photoswitchable polymerization



106 **Fig. 2 | Different types of switchable catalysis as temporal control.** a | Switchable catalysis using different external  
107 stimuli. b | Redox-switchable catalysis. (i) Design of a redox-switchable metal catalyst. (ii) Redox-switchable  
108 polymerization using electrochemical setup. Fe(II) catalyst can polymerize lactide (red ball) while the Fe(III) catalyst  
109 can polymerize cyclohexene oxide (green ball). c | Chemoswitchable catalysis. (i) Anion coordination leads to  
110 allosteric change which unblocks the catalytic active center for the ring opening polymerization of  $\epsilon$ -caprolactone.  
111 The red block denotes a bulky aromatic group that results in steric hindrance. (ii) Metal cation coordination onto the  
112 hemilabile crown ether moiety promotes the hydrogen activation reaction. (iii) Metal cation coordination to the  
113 oligomeric ethylene glycol chain increases ethylene polymerization activity. (iv) Presence of CO<sub>2</sub> prevents the  
114 polymerization of  $\epsilon$ -caprolactone (blue ball) and initiates the ring opening copolymerization of CO<sub>2</sub> and cyclohexene  
115 oxide (green ball). d | Photoswitchable catalysis. (i) The catalyst can bind to the substrates via hydrogen bonds; in  
116 the E form the catalyst can bring the substrates closer and accelerate the amidation process, while the Z form  
117 separates the substrates apart and thus slows down the amidation. (ii) The diarylethene-type catalyst with a phenol  
118 moiety in the ring-opened phenol form incorporates more valerolactone (blue ball) while the ring-closed ketone  
119 form incorporates more trimethylene carbonate (purple ball) in the copolymerization process. (iii) By using different  
120 photocatalysts and changing the wavelength of light, the polymerization mechanism can switch between radical and  
121 cationic polymerization.

122

### 123 [H3] Redox-switchable catalysis

124 A challenge associated with achieving switchable catalysis is designing a system that has two (or more)  
125 different reactive states that can be accessed through application of external stimuli. Since redox reactions  
126 change the electronic configuration of a compound, which is intimately associated with its reactivity, an  
127 attractive option for switchable catalysts is through iterative addition of oxidants or reductants. A  
128 common way to carry out **redox-switchable catalysis** [G] is to design redox-active ancillary ligands<sup>44-46</sup> that  
129 are coordinated to a redox-inactive metal, which serves as the site for catalysis. This strategy was  
130 employed in the first example of redox-switchable catalysis,<sup>47</sup> when a rhodium complex supported by a  
131 cobaltocene bis(phosphine) was used for the hydrogenation and isomerization of alkenes. Despite this  
132 first example being applied to catalysis involving small molecules, the utility of redox-switchable catalysis  
133 has been exploited with more success in polymerization. For example, a titanium complex containing two  
134 redox-active ferrocene moieties appended to a salen (N,N'-bis(salicylidene)ethylenediamine) ancillary  
135 ligand (FIG. 2bi)<sup>48</sup> demonstrated redox modulation when used for the polymerization of lactide, with the  
136 reduced species being more active than the oxidized form of the catalyst. Since this report, several groups  
137 have utilized the ferrocene moiety for redox-switchable polymerization.<sup>49-54</sup> For example, using chelating  
138 ligands to position the ferrocene moiety in close proximity to the redox-inactive site for catalysis results  
139 in a greater difference in the reaction rate of the oxidized and reduced states of a catalyst (FIG. 2b). For  
140 example, while both forms of the above titanium complex demonstrated some activity for lactide  
141 polymerization, an yttrium complex showed complete on/off activity for lactide polymerization.<sup>55</sup>

142 An alternative method for redox-switchable catalysis is to use redox-active metals that serve as the redox-  
143 switching moiety and the site for catalysis (FIG 2bi). Catalysts based on several different redox-active  
144 metals have been explored using this strategy, with the most notable examples being ring-opening  
145 polymerization catalysts using cerium salen<sup>56</sup> and iron bis(imino)pyridine complexes.<sup>57</sup> These catalysts

146 show similar behavior as that of polymerization catalysts utilizing redox-active ancillary ligands,  
147 demonstrating that it is not necessary to separate the redox-switching entity from the catalytically active  
148 entity.

149 A challenge associated with redox-switchable catalysis is the need to add oxidants and reductants to the  
150 reaction. When chemical redox reagents are used, purification of the product is required to remove the  
151 byproducts from the redox-switch. Moreover, adding chemical redox reagents to reactions that require  
152 gaseous reagents at elevated pressures requires specialized equipment. To address these limitations, an  
153 electrochemical potential can be used instead of chemical redox reagents for redox switching (FIG. 2bii).  
154 Such electrochemical potential can be achieved by employing bis(imino)pyridine iron complexes whose  
155 redox-active site is also the site for catalysis,<sup>58</sup> or catalysts that contain redox-switchable moieties installed  
156 in the ancillary ligand.<sup>59</sup>

157 While there are now many redox-switchable catalysts, a mechanistic understanding of how these systems  
158 perform redox switching is not well established. The oxidation state of the active catalyst and the  
159 efficiency of the redox switch are dependent on many factors. In addition to the proximity of the redox-  
160 switching moiety to the catalytically active site, another important factor is the identity of the metal center.  
161 For example, while the yttrium complex is active for lactide polymerization in its reduced state, the indium  
162 complex that contains the same ancillary ligand is active for lactide polymerization in its oxidized state.<sup>55</sup>  
163 The interaction between the metal center and the redox switchable moiety can be intricate; as revealed  
164 by computational and experimental studies,<sup>60,61</sup> the oxidation state of the redox active group can alter the  
165 Lewis acidity of the metal center, as well as change the energetic profile of the catalyst-substrate  
166 interaction.<sup>62</sup> Another factor is the identity of the reactant; some reactants may display orthogonal  
167 reactivity with respect to the oxidation state of the catalyst and some may not. For example, the iron  
168 complex shown in FIG. 2bii,<sup>63</sup> as well as other redox switchable catalysts,<sup>51,53,55,60,64,65</sup> is capable of  
169 polymerizing lactide selectively in its reduced form and epoxide in its oxidized form, but less selectivity is  
170 observed for lactones or cyclic carbonates.<sup>61,64,66-68</sup> The selectivity shown by each state of the system, i.e.,  
171 orthogonal reactivity, is important in being able to combine multiple catalytic cycles without interference  
172 from the reaction that is turned off, for example. While more work is needed to understand these and  
173 other effects, two related factors appear to be important in polymerization catalysis: the propensity of  
174 the monomer to bind to the catalytically active site and the electrophilicity/nucleophilicity of reactive  
175 intermediates.<sup>61,67,69</sup> Both factors are altered by changing the oxidation state of the catalysts, and the  
176 relative importance of each is related to the nature of each reaction, including the identity of the metal  
177 centers and the monomers employed.

178

## 179 [H2] Chemoswitchable catalysis

180 Chemoswitchable catalysts are compounds that are responsive to the presence of external chemical  
181 additives. Unlike redox-switchable catalysis, chemoswitchable catalysis [G] does not involve alterations to  
182 the catalyst that leads to changes in their formal oxidation state. Because chemical reagents have a wide  
183 range of properties, they can trigger molecular events via various modes of action. For example, cations

184 can bind Lewis basic sites, whereas anions can bind Lewis acidic sites. Such interactions could turn a  
185 catalyst on or off, or modulate their reaction rates. Alternatively, chemical reagents could covalently  
186 modify a catalyst to produce another active species capable of achieving orthogonal reactivity.

187 The key design challenge in chemoswitchable catalysis is to enable a catalyst to change its structure and  
188 function by interacting with a chemical additive. One effective strategy for chemoswitchable reactivity  
189 involves regulating catalysis using anion coordination/dissociation to alter the metal complex geometry  
190 or block/unblock catalytically active sites. For instance, a supramolecular triple layer catalyst, comprising  
191 an aluminum salen complex flanked by two rhodium nodes equipped with biaryl blocking groups, was  
192 used for the chemoswitchable polymerization of lactones (FIG. 2ci). In the closed form, the rhodium  
193 centers are ligated by the amino donor of the supporting ligand, which positions the biaryl units above  
194 and below the aluminum active site.<sup>70</sup> Because aluminum is inaccessible due to the steric bulk of the  
195 amino arms, the catalyst cannot react with substrates. In the open form, chloride anions are bound to  
196 rhodium so that the amino groups are forced away from aluminum, opening up access to incoming  
197 monomers. When chloride salts are added, the triple layer catalyst reaches an open state that is active  
198 for the ring-opening polymerization of  $\epsilon$ -caprolactone; when sodium salts are added, the chloride is  
199 abstracted from the rhodium centers, re-forming the closed catalyst state and almost completely stopping  
200 the polymerization. Remarkably, the molecular weight of the polymer increased linearly with conversion  
201 even as the catalyst was activated, deactivated, and reactivated, indicating an excellent control over  
202 catalysis.

203 Another strategy for chemoselective switching is to regulate catalysis using cations. By installing crown  
204 ether moieties in ancillary ligands, alkali metal cations can interact with the crown ether moiety to tune  
205 the electron density of the catalytically active site. This type of cation switching has been well-  
206 demonstrated in small molecule activation (FIG. 2cii).<sup>71</sup> For example, an iridium PCN-pincer complex was  
207 prepared containing an aza-crown ether macrocycle, which serves as a hemilabile ligand and cation  
208 receptor. When sodium or lithium tetraarylborate salts were added to a  $CD_2Cl_2/Et_2O$  solution of the  
209 compound, the free energy of aza-crown ether dissociation from iridium is lowered due to the favorable  
210 interaction of the alkali metal ion with the macrocycle. In the presence of these alkali metal cations,  
211 binding of dihydrogen becomes possible, and the cation-activated iridium species catalyzed H/D exchange  
212 with  $D_2$  is significantly faster than the unactivated complex. This concept can be extended to a three-state  
213 (off/slow/fast) catalyst system, such as the positional olefin isomerization.<sup>72</sup> For example, iridium chloride  
214 complex is inactive for isomerization of allylbenzene; removal of the chloride produces a cationic species  
215 with hemilabile Ir–O interactions resulting in a slow catalyst. Addition of  $Li^+$  salts to this cationic catalyst  
216 enhances the isomerization rate over 1,000-fold. The rate enhancement is attributed to cation–crown  
217 interactions making olefin binding more favorable, and increasing the amount of iridium that is actively  
218 engaged in catalysis. Another example of a cation-switchable system was used to achieve regioselectivity  
219 in positional isomerization: without salts added, alkenes were isomerized from the 1- to the 2-position;  
220 under the same conditions but with added  $Na^+$  salts, 3-alkenes were observed instead.<sup>73</sup>

221 The cation coordination strategy of a catalyst can be used to tune not only the reaction rates but also the  
222 architecture of a polymer product.<sup>74</sup> For example, a family of nickel phenoxyimine complexes bearing

223 polyethylene glycol (PEG) chains can coordinate secondary metals (FIG. 2ciii); the addition of  $M^+$  (where  
224  $M^+ = Li^+, Na^+, \text{ or } K^+$ ) can produce 1:1 and 2:1 nickel: alkali species. The association constants between Ni  
225 and  $M^+$  correlated with the size match between the ionic radius of  $M^+$  and the chain length of the PEG  
226 chelator (larger cations require longer PEG chains and vice versa). Combining  $Na^+$  or  $K^+$  with the nickel  
227 catalysts featuring tri- or tetra-ethylene glycol chains increased the ethylene polymerization activity and  
228 gave polymers with higher molecular weight and branching density than the nickel catalysts alone. Cation-  
229 tuning was also applied to other olefin polymerization platforms and catalyst nuclearity was controlled  
230 through suitable ligand design.<sup>75-78</sup>

231 Small gas molecules can also be utilized as chemoselective switches by serving either as a trigger or a  
232 substrate for a reaction. For example,  $CO_2$  can be used to oscillate a catalytic system between ring opening  
233 polymerization [G] (ROP) of a lactone and ring opening copolymerization (ROCOP) of epoxides and  $CO_2$   
234 (FIG. 2civ).<sup>79,80</sup> Another example of a small gas molecule switch is  $O_2$ . Although more well-known as a  
235 radical scavenger,  $O_2$  can also be used in chemical transformations to generate radical species that can  
236 initiate radical polymerization.<sup>81,82</sup> Small gas molecules have the advantage of being easy to remove,  
237 however, a pressure reactor might be needed for the reaction.

238 Such examples demonstrate that chemical switching can be a useful strategy for regulating many different  
239 catalytic processes. Chemical switching can also take advantage of solution equilibria to tune reaction  
240 rates in a dynamic fashion. In cation tuning, different amounts or types of metal salts can be used to  
241 achieve different effects without requiring tedious synthetic modifications of the catalyst. Ideally, the  
242 chemical switch is only needed in catalytic amounts relative to the substrate (for example, in cation  
243 switching) or is incorporated into the reaction product (such as in CHO and  $CO_2$  ROCOP). Some possible  
244 disadvantages of chemical switching are that the chemical reagents used are not traceless so they may  
245 need to be removed from the final product or they might not be compatible with subsequent steps in  
246 one-pot tandem or cascade reactions. Another potential limitation in cation switching is that the catalyst  
247 must be amenable to installation of secondary metal binding groups to achieve high cation responsiveness  
248 since Lewis acid additives are relatively commonly used to enhance activity.<sup>83</sup>

249

### 250 [H3] Photoswitchable catalysis

251 Photoresponsive processes are ubiquitous in nature and in artificial synthesis and catalysis.  
252 Photoswitchable catalysis involves a catalytically active species that can undergo a reversible  
253 photochemical transformation, which consequently changes its intrinsic catalytic properties.<sup>84</sup> In  
254 photoswitchable catalysis, photochromic functionalities such as azobenzenes, which can undergo an E-Z  
255 isomerization, and diarylethenes, which can undergo a photo-induced ring closing, are commonly  
256 employed.

257 The photoinduced E-Z isomerization of diarylethenes and stilbenes can lead to a change in the steric  
258 environment of the active site, which can block or unblock substrate access or bring substrates closer  
259 together or further apart, thus changing the catalytic activity.<sup>85</sup> Such azobenzene photochromic  
260 functionality has been used to control the rate of an amidation reaction (FIG. 2di).<sup>86</sup> For example, for the

261 amidation between aminoadenosine and adenosine-derived *p*-nitrophenol ester, a template molecule  
262 that contains two adenine receptors linked by an azobenzene spacer was designed. When the template  
263 molecule is in the E configuration, substrates bound to each receptor are far apart, resulting in a slow  
264 coupling rate. Upon UV irradiation ( $\lambda_{\text{ex}} = 366 \text{ nm}$ ), the template molecule undergoes a photo-induced  
265 isomerization, resulting in a photostationary state ratio of E:Z = 1:1. The Z configuration brings the two  
266 substrates in close proximity, thereby accelerating the reaction.

267 The photoinduced ring opening or ring closing of photochromic functionalities, such as spiropyrans<sup>87,88</sup>  
268 and diarylethenes,<sup>89</sup> results in steric and electronic changes that have been used to alter rates of lactone  
269 polymerization. For example, in a diarylethene-based system (FIG. 2dii),<sup>90</sup> the ring-opened phenol catalyst  
270 uses the exposed -OH group to activate lactide, which leads to a high polymerization rate. Upon UV  
271 irradiation ( $\lambda_{\text{ex}} = 300 \text{ nm}$ ), a photostationary state is reached, leading to 98% of the ring-closed ketone  
272 isomer, which shows a diminished polymerization rate. The system can be turned back on to the active  
273 state by irradiation with visible light. The different rates of the opened and closed forms toward  
274 valerolactone and trimethylenecarbonate (TMC) polymerization can also be harnessed to control the  
275 microstructure of the polymers. The ring-opened phenol catalyst, incorporates more valerolactone than  
276 TMC to synthesize copolymers with higher valerolactone content, while the ring-closed ketone isomer  
277 leads to a polymer with higher TMC than valerolactone content.

278 Unlike most redox-switchable and chemoswitchable catalysts, photoswitchable catalysis provides a non-  
279 invasive method to achieve temporal control since light is the only reagent required for switching.  
280 Consequently, product purification does not require removing excess reagents. Additionally, switching  
281 can be fast and not limited by mass transport.<sup>91,39,92</sup> A combination of different polymerization  
282 mechanisms can also be achieved by changing the wavelengths of light. For example, by using  
283 photocatalysts and a thiocarbonate chain transfer agent, cationic polymerization could be initiated by  
284 green light, while radical polymerization could be commenced by blue light (FIG. 2diii).<sup>93</sup> In terms of the  
285 experimental setup, light-emitting diodes are typically used as a source of light with specific and narrow  
286 wavelength. Although photoswitchable catalysis shows many advantages in temporal control, it also  
287 needs to overcome several hurdles such as obtaining a high photostationary state isomer ratio with a  
288 short irradiation time, finding isomers with orthogonal reactivity, and using UV light, which limits  
289 compatibility with some organic substrates or metal catalysts.

290

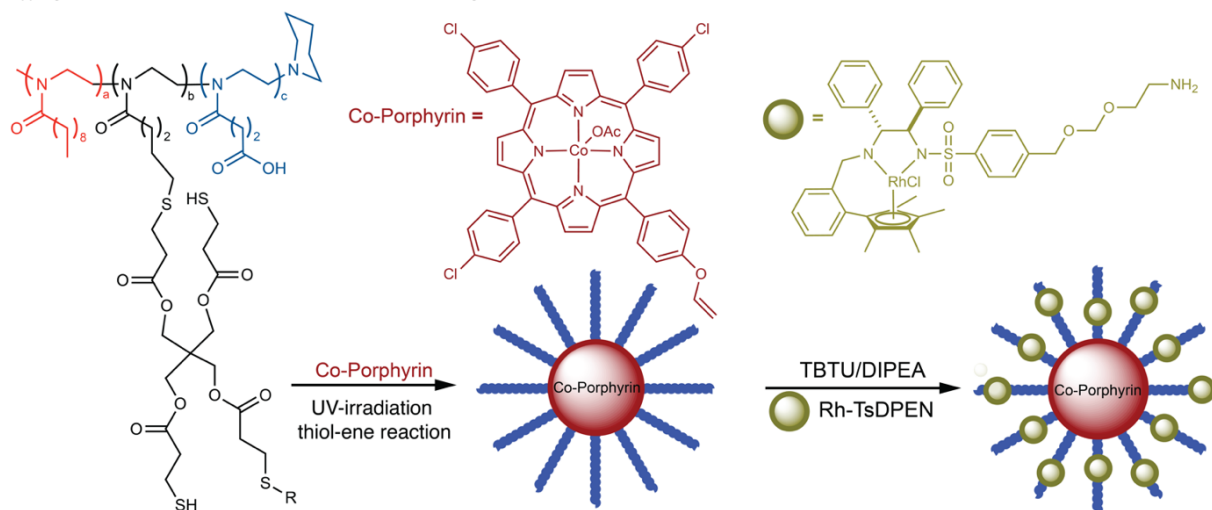
## 291 [H2] Spatial control

292 Spatial control in catalysis refers to the localization or separation of a catalyst from other species in  
293 reaction media. There are many reasons why spatial control is desirable, ranging from mitigating  
294 incompatibility between reagents/catalysts<sup>8,13,18,20,21,23-27,94-99</sup> to simple heterogenization of a catalyst to  
295 be recycled,<sup>23,100-107</sup> and opportunities to capitalize on local concentrations of reagents and effects that  
296 may occur from local magnetic or electric fields.<sup>20,37,108-110</sup> Spatial control may be realized in numerous  
297 ways, with the bulk of this work centered around confining catalysts within compartments,<sup>8,13,20,23,25-27</sup>  
298 using biphasic conditions,<sup>111-114</sup> and immobilizing catalysts onto supports.<sup>100-103</sup> The last few decades have

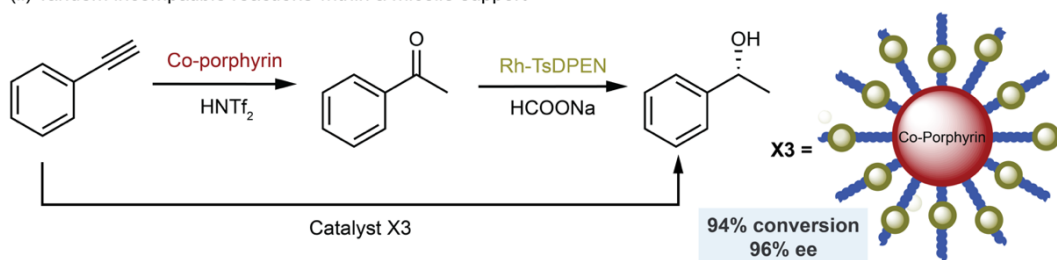
299 witnessed a steady growth in exploring the spatial control of molecular catalysts, with several reviews  
 300 outlining the intricacies and caveats of localizing catalysts.<sup>23,26,97,100</sup> Here, the motivations and working  
 301 principles for spatial control are discussed, all within the context of ultimately utilizing spatial localization  
 302 to control multiple catalysts in proximity and circumvent potential challenges in integrating catalysis to  
 303 carry out catalytic transformations that are not trivial for homogeneous catalysts.

### a Compartmentalization of two catalysts in micelles

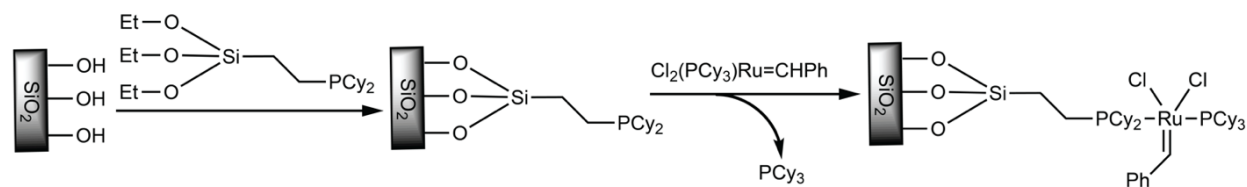
(i) Synthetic scheme for micelle formation and catalyst confinement



(ii) Tandem incompatible reactions within a micelle support



### b Catalyst immobilization onto an oxide support



304  
 305 **Fig. 3 | Approaches to spatial control via compartmentalization of catalysts in close proximity within confined**  
 306 **spaces.** a | (i) Micelle support with the synthetic scheme for micelle formation. An amphiphilic ABC-triblock  
 307 copolymer was used to form the micelle support. The cobalt catalyst was covalently attached to the hydrophobic  
 308 core (red and black blocks) via the thio-ene reaction, while the rhodium catalyst was attached to the hydrophilic arm  
 309 (blue block). (ii) Tandem alkyne hydration and hydrogenation. b | Immobilization of two species in close proximity  
 310 onto an oxide surface for synergistic catalysis.

311

### 312 [H3] Compartmentalization

313 Two major forms of spatial control are compartmentalization and **surface immobilization [G]**. The key  
314 challenge in compartmentalization is to design a system that keeps each catalyst inside a specific  
315 compartment while allowing reactants, intermediates, and products to move between the compartments.  
316 Compartmentalization has been reported in the biocatalytic literature as an approach for constructing  
317 efficient tandem catalysis by separating enzymes in well-defined micro- and nano-structures.<sup>21,22,115-119</sup> In  
318 doing so, compartmentalization results in beneficial circumvention of deactivating or competing pathways,  
319 retention of reactive or toxic intermediates, increases in reaction rates and high local substrate  
320 concentration.<sup>21,22,115-119</sup> Inspired by the mechanistic work on in vivo compartmentalization, spatial  
321 organization at the nano- and microscopic levels has been implemented to construct in vitro biomimetic  
322 cascades with augmented catalytic performance.<sup>22,26,95,99,117,120,121</sup> For example, confining the  $\beta$ -galactose,  
323 glucose oxidase, and horseradish peroxidase in metal-organic frameworks led to an enhancement of the  
324 reaction yield in comparison to a freely diffusing enzyme.<sup>26,95</sup> Additionally, encapsulation of a nickel-iron  
325 hydrogenase in capsids enhanced the rate of H<sub>2</sub> production and improved the enzyme's thermal  
326 stability.<sup>121</sup>

327 Following the wealth of literature in applications of bio-compartmentalization, the organometallic  
328 community has subsequently made great strides in confining transition metal-based catalysts. Of  
329 relevance to integrated catalysis, compartmentalization may be used to construct efficient tandem,  
330 heterogeneous, organometallic systems that otherwise cannot be achieved with homogeneous  
331 catalysts.<sup>8,13,18,20,27</sup> The majority of prior confined organometallic catalysts focuses on employing  
332 macromolecular structures to tune selectivity in a manner unachievable in a homogeneous setting.<sup>23</sup>  
333 Additionally, the confinement of such catalysts often results in an improved stability and heightened  
334 activity over freely diffusing analogues.<sup>23</sup> Furthermore, compartmentalization has been applied to  
335 organometallic-mediated catalytic chain transfer polymerization, from which insight into the relationship  
336 between confinement and polymer modality has been extensively studied.<sup>122-124</sup>

337 Organometallic catalyst(s) can be compartmentalized by encapsulation in molecular cages to accelerate  
338 reaction rates and alter selectivity.<sup>23,125-129</sup> One example of compartmentalization is the selective  
339 recognition and stabilization of imminium ions by a Ga(III) catecholate molecular cage.<sup>130</sup> The  
340 compartmentalization of catalysts in molecular cages has been extensively applied in various reactions,  
341 such as aza-Prins cyclizations,<sup>131</sup> to promote kinetically disfavored pathways and thus steer selectivity.<sup>131</sup>  
342 One way to do this is using a micelle to support two co-encapsulated catalysts for incompatible catalytic  
343 reactions (FIG. 3a).<sup>8</sup> For example, in the direct conversion of an alkyne to an enantioenriched secondary  
344 alcohol, the Co-porphyrin catalyzed hydration of alkyne to ketone was not compatible with the Rh-TsDPEN  
345 catalyzed asymmetric hydrogenation of ketone to secondary alcohol, and when the two catalytic reactions  
346 were carried out in tandem, no product was detected. To bypass the issue, the cobalt catalyst was  
347 immobilized in the hydrophobic core of the micelle and the rhodium catalyst in the hydrophilic shell thus  
348 separating the two catalytic systems in two different domains to avoid interference. The intra-micellar  
349 diffusion of the ketone intermediate was fast enough to render high efficiency to the overall reaction.

350 Changing the local environment of a catalyst may understandably alter its catalytic properties, such as  
351 activity. Thus, in the realm of confinement via compartmentalization, a judicious design and choice of  
352 compartments will be paramount.<sup>132</sup> A likely pitfall of this approach may be a deleterious reduction in  
353 activity. To circumvent this, we point out a recent report that modeled the effect of varying compartment  
354 dimensions on catalytic activity for several common catalytic cycles.<sup>27</sup> Ultimately, a confinement must be  
355 employed carefully so that entry and exit into the compartment via diffusion is as fast as or slower than  
356 the kinetics of the catalytic cycle.

357

### 358 [H3] Surface immobilization

359 Another way to achieve spatial control over a reaction is by attaching a molecular catalyst onto a solid  
360 support material, also known as **surface immobilization [G]**.<sup>28,30-35,133-135</sup> A rich history of surface  
361 attachment of catalysts has led to a diverse lexicon: a compound can be attached, anchored, or  
362 immobilized to produce a surface-supported or surface-immobilized catalyst. Sometimes such systems  
363 are referred to as single-site heterogeneous catalysts because, ideally, the molecular nature of the catalyst  
364 leads to excellent homogeneity in catalyst activity and selectivity, while also boasting the benefits of a  
365 heterogeneous catalyst (for example, easy separation from reactants/products, facile recycling). An  
366 immobilized catalyst will only carry out the reaction where it is anchored to the surface, controlling the  
367 location of product generation. Furthermore, two or more catalysts can each be attached to a surface in  
368 order to prevent unwanted interactions and ensure catalyst compatibility, an invaluable aspect in  
369 integrated catalysis. For example, a palladium catalyst and an organic base were co-immobilized in close  
370 proximity onto a silica surface (FIG. 3b).<sup>136-138</sup> Synergism was realized by a significant acceleration (3 times  
371 higher conversion) of palladium catalyzed Tsuji–Trost allylic alkylation reactions with the co-immobilized  
372 palladium catalyst and organic base material, in comparison to a palladium catalyst on the silica surface  
373 without an organic base pair in close proximity.<sup>136</sup> In integrated catalysis, this approach may be adapted  
374 to co-immobilize two incompatibly catalysts, such as a metal/enzyme system,<sup>139,140</sup> to minimize transport  
375 between catalyst sites, while preventing deleterious interactions between them.

376 Considering the breadth of methods for surface attachment, ranging from covalent bonding to a silica  
377 surface or non-covalent interactions with modified surfaces,<sup>28-35,133-135,141-143</sup> the following should be  
378 considered when designing an anchored catalyst system. First, the application is important. Thermal  
379 reactions require a support that is robust under the reaction conditions, whereas electrochemical  
380 reactions require a conductive support and a linker that provides sufficient electronic coupling.  
381 Photochemical reactions generally require a transparent support, and often materials with a high surface  
382 area so that a sufficient amount of photocatalyst can absorb light. Second, the reaction mechanism is  
383 relevant. If multiple catalysts are required, the anchoring group should be sufficiently long and flexible to  
384 accommodate intermolecular interactions. If ligands dissociate, then the dissociating ligands should not  
385 be chosen for the attachment group to avoid catalyst leaching. Third, the reaction solvent is also important.  
386 Sequestration methods that rely on weak intermolecular forces, such as hydrophobic interactions, may  
387 be appropriate for reactions in water but not reactions that require nonpolar solvents. Finally, in terms of

388 the synthetic strategy to be used, sometimes it is more effective to anchor an organic group with a key  
389 functionality, and then use a different reaction to anchor the metal unit. For example, a silyl ether  
390 containing an azide can be attached to a surface, and then an alkyne-containing metal complex can be  
391 connected to the azide in a copper-catalyzed click reaction to form a robust linkage.<sup>35</sup>

392

## 393 [H2] Biocatalysis

394 Biocatalysis has become a vital component in modern organic synthesis, spanning from academic research  
395 to industrial chemical and pharmaceutical processes.<sup>144</sup> Natural enzymatic catalysis is remarkable in its  
396 high activity and selectivity and mild working conditions. Although naturally evolved enzymes typically  
397 have a limited substrate scope, their performance may be enhanced by artificial enzyme engineering or  
398 integration with chemocatalysis for broader applications.<sup>145</sup> For instance, in dynamic kinetic resolution of  
399 amines and alcohols, an enantioselective enzyme catalyst was coupled with a racemization catalyst to  
400 maximize the reaction yield.<sup>104</sup> Furthermore, the spatial and temporal control methods developed for  
401 synthetic catalysis could also be applied to biocatalysis, providing new strategies to manipulate enzymes.  
402 For example, the integration of biocatalysis and photoredox catalysis has been developing rapidly in  
403 recent decades enabling otherwise challenging chemical transformations.<sup>146,147</sup> Spatial control approaches  
404 such as immobilizing enzymes onto heterogeneous supports<sup>148</sup> and crosslinking enzymes to form  
405 extended structures<sup>149,150</sup> can simplify the workup process and facilitate enzyme recycling.

406 Biology has many exquisite examples of systems that can manage complex reaction networks and perform  
407 efficient multistep reaction sequences.<sup>21,24-26,95,96,116,117,119,120,151,152</sup> Compartmentalization is a key spatial  
408 control feature that allows organelles to orchestrate how enzymes and substrates/intermediates interact,  
409 while simultaneously blocking entry of unwanted species. Discussed previously, compartmentalization is  
410 a major form of spatial control that biology also utilizes, wherein meticulously designed organelles localize  
411 enzymes and key substrates in close proximity to allow efficient channeling of intermediates between  
412 active sites, while simultaneously blocking entry of unwanted or exit of wanted intermediate species into  
413 or out of the confinement.<sup>151,152</sup>

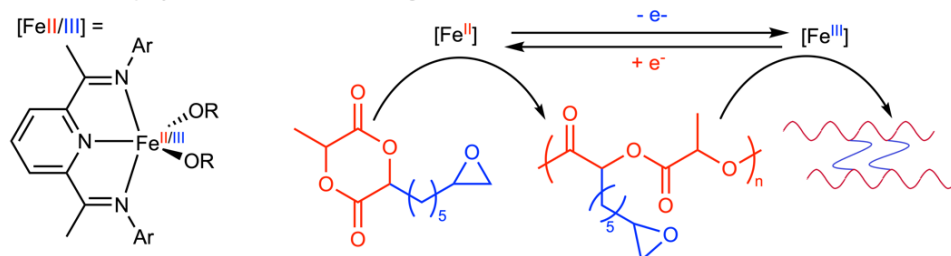
414 A representative example is the co-encapsulation of glucose oxidase and horse radish peroxidase within  
415 macromolecular scaffolds such as MOFs or polymersomes.<sup>26,153</sup> The cascade sequence between the two  
416 enzymes that consumes glucose shows drastically improved yields when the enzymes are confined versus  
417 the freely diffusing analogues. This method has been applied to many multi-enzyme systems,  
418 demonstrating that it is a robust strategy for creating complex yet efficient catalytic processes. Temporal  
419 control methods are also commonly used in biocatalysis, such as applying actuators or substrate gates to  
420 direct when each step of multienzymatic processes occurs.<sup>154,155</sup> The combination of enzymes with  
421 synthetic catalysts offers the best of both worlds, providing new opportunities to streamline chemical  
422 synthesis.<sup>156</sup>

423

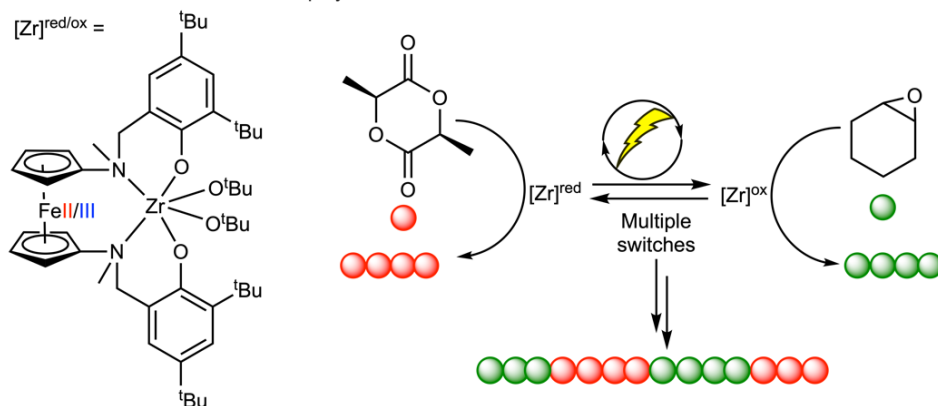
424

## a Switchable catalysis in polymer microstructure control

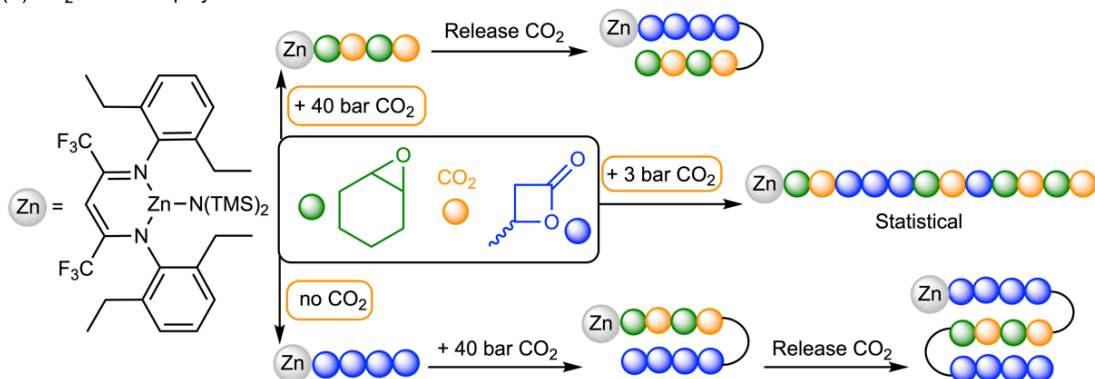
(i) Redox switchable polymerization and crosslinking



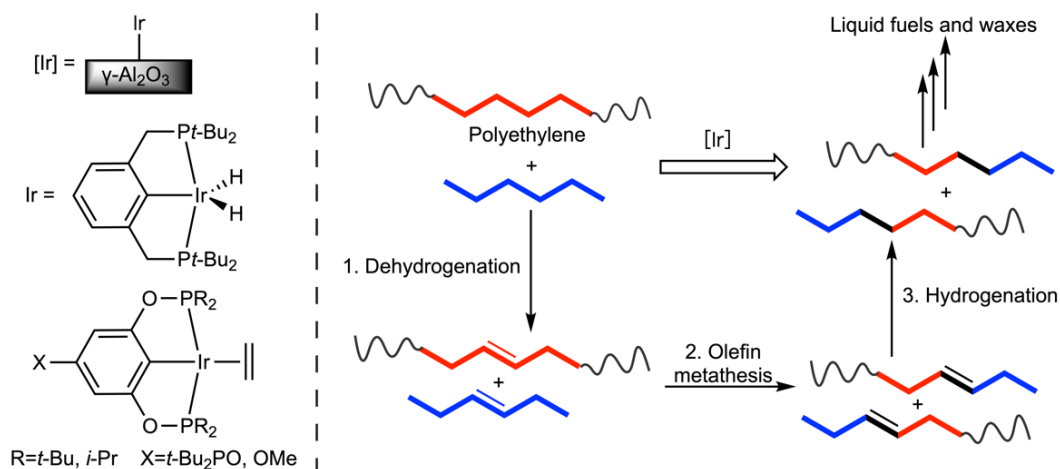
(ii) Electrochemical redox switchable polymerization



(iii) CO<sub>2</sub> controlled polymerization



## b Polyethylene degradation by supported Ir catalyst



426 **Fig. 4 | Temporal and spatial control in integrating different catalytic cycles.** a| Harnessing activity of different  
427 catalytic states to control the polymer sequence and microstructure. (i) Redox-switchable catalysis toward the  
428 synthesis of a biodegradable crosslinked polymer network. (ii) Electrochemically controlled redox-switchable  
429 polymerization to synthesize a tetrablock copolymer. b| Polyethylene degradation via tandem (de)hydrogenation  
430 using  $\gamma$ -Al<sub>2</sub>O<sub>3</sub> supported iridium complexes and alkane metathesis using Re<sub>2</sub>O<sub>7</sub>/Al<sub>2</sub>O<sub>3</sub>. The dehydrogenation/  
431 hydrogenation process was catalyzed by the iridium compound while the olefin metathesis step was catalyzed by  
432 Re<sub>2</sub>O<sub>7</sub>/Al<sub>2</sub>O<sub>3</sub>.

433

## 434 [H2] Addressing catalytic compatibility

435 Spatial and temporal control approaches provide the means for coupling multiple catalytic cycles in a  
436 single reaction vessel. Spatiotemporal control may be utilized to couple different catalytic cycles by either  
437 exploiting the switchable catalysis of a single precatalyst or by reconciling incompatibility among multiple  
438 catalytic systems to generate products that would otherwise be difficult to synthesize. In this regard,  
439 polymerization reactions are the best examples to showcase how complex products can be generated  
440 from simple building blocks.

### 441 [H3] Cross-linking

442 Cross-linked polymer networks are valuable materials due to their high toughness and enhance thermal  
443 properties.<sup>157,158</sup> These materials are often synthesized using two-part resins or through the application of  
444 heat or light as a trigger for cross-linking. Each of these methods have different limitations such as the  
445 temperature required for heating and limited substrate penetration, respectively. The orthogonal activity  
446 of redox-switchable catalysis can be applied in the realm of polymer crosslinking to address some of these  
447 limitations (FIG. 4ai).<sup>159</sup> For example, when a bifunctional monomer that contained a cyclic diester and a  
448 pendant epoxide was polymerized upon exposure to an iron(II) complex, an epoxide-functionalized  
449 polyester was formed. By adding an external oxidizing agent, Fe(II) is oxidized to Fe(III), triggering the ring-  
450 opening polymerization of the epoxide moiety, thereby forming a crosslinked polymer network.  
451 Compared to linear poly(lactic acid), the cross-linked polymers show remarkably different thermal and  
452 physical properties. Moreover, the crosslinking method that capitalizes on the switching capability of the  
453 iron complex is beneficial because it does not require two-part resins, polymer creep is not an issue, and  
454 there are no limitations with respect to the thickness of substrates.

### 455 [H3] Switchable polymerization

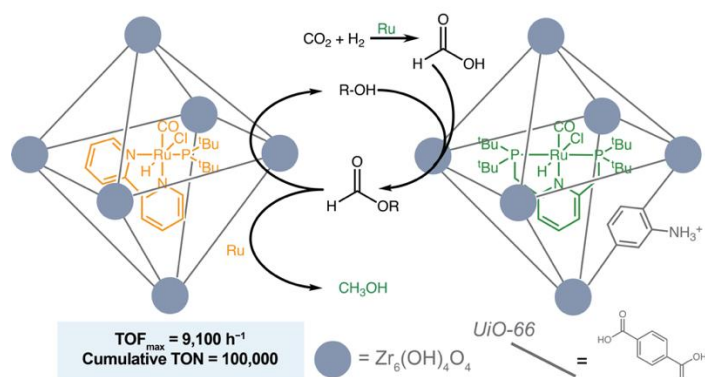
456 Other sophisticated macromolecules can be synthesized by taking advantage of switchable  
457 polymerization reactions, such as block copolymers. Block copolymers demonstrate very useful properties  
458 by melding the properties of two different polymer classes. However, some block copolymers cannot be  
459 synthesized through sequential addition of monomers because the mechanisms for their polymerization  
460 may be very different. Consequently, these block copolymers are usually synthesized through sequential  
461 polymerization reactions that sometimes involve tedious and imperfect post-polymerization chain-end  
462 modifications to accommodate subsequent reactions. When encountering this scenario, switchable  
463 polymerization reactions are a good option to allow for the synthesis of block copolymers from pools of

464 monomers in a single reaction vessel. Electrochemistry has advanced redox-switchable catalysis by  
465 obviating the need for chemical oxidants and reductants, thus bypassing the incompatibility issue  
466 between substrates and redox reagents when the reaction is conducted in one pot. As such,  
467 electrochemically controlled redox-switchable catalysis have been employed to synthesize block  
468 copolymers in one pot.<sup>58,59</sup> For example, a ferrocene-containing zirconium compound is active in its  
469 reduced state for lactide polymerization, but inactive for epoxide polymerization (FIG. 4a<sub>ii</sub>). When  
470 oxidized, the activity is reversed toward these two types of monomers. To achieve the synthesis of a  
471 multiblock copolymer, a one-pot setup was used with lactide and cyclohexene oxide monomers present  
472 at the beginning of the reaction to simplify the overall process, and electrochemistry was used to eliminate  
473 the need to add reagents during copolymerization. Using this strategy, a tetrablock copolymer was  
474 synthesized through sequential application of oxidative and reductive potentials. In addition to simplifying  
475 polymer purification, the electrochemical setup precludes possible side reactions, such as epoxide  
476 polymerization initiated by oxidants.

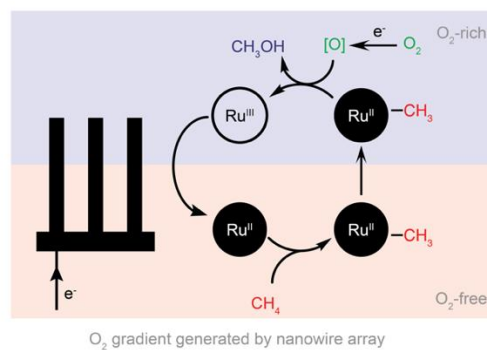
### 477 [H3] Solid supports

478 Spatially localizing a catalyst on the surface of a silica support is another important method that can be  
479 used to address compatibility issues. Although the general perception is that immobilizing the catalyst  
480 onto a surface reduces its activity due to hindered mass transport, the activity loss can be compensated  
481 with appropriate system modifications and optimization. For example, when various  $\gamma$ -Al<sub>2</sub>O<sub>3</sub> supported  
482 iridium complexes (Ir@ $\gamma$ -Al<sub>2</sub>O<sub>3</sub>) used for alkane dehydrogenation and alkene hydrogenation were  
483 combined with a heterogeneous alkene metathesis catalyst (Re<sub>2</sub>O<sub>7</sub>/Al<sub>2</sub>O<sub>3</sub>), polyolefin degradation was  
484 observed when the polymer was combined with a light alkane (FIG. 4b).<sup>160</sup> By carrying out the alkane  
485 dehydrogenation in tandem with the olefin metathesis, alkanes are converted into substrates for alkene  
486 metathesis, the products from which are substrates for hydrogenation, thereby resulting in new alkanes.  
487 When the polymeric alkane polyethylene is combined with an excess of a light alkane, the result is smaller  
488 alkanes. Importantly, the dual nature of the iridium complexes used for alkane dehydrogenation and  
489 alkene hydrogenation enables the process, and requires that the supported iridium complex be used  
490 concurrently with the heterogeneous metathesis catalyst. Moreover, separating the molecular iridium  
491 complexes from the rhenium alkane metathesis catalyst circumvents any unwanted catalyst-catalyst  
492 interactions, which plagued similar reactions involving entirely homogeneous catalysts.<sup>6</sup> In addition, this  
493 system proved effective even when commercial polyethylene products, such as plastic bottles and food  
494 packaging were employed. This approach has also been employed in alkane upgrading by both homo- and  
495 heterogeneous Ir species,<sup>161</sup> the olefin degradation exemplified discussed shows spatial control of multiple  
496 catalysts.

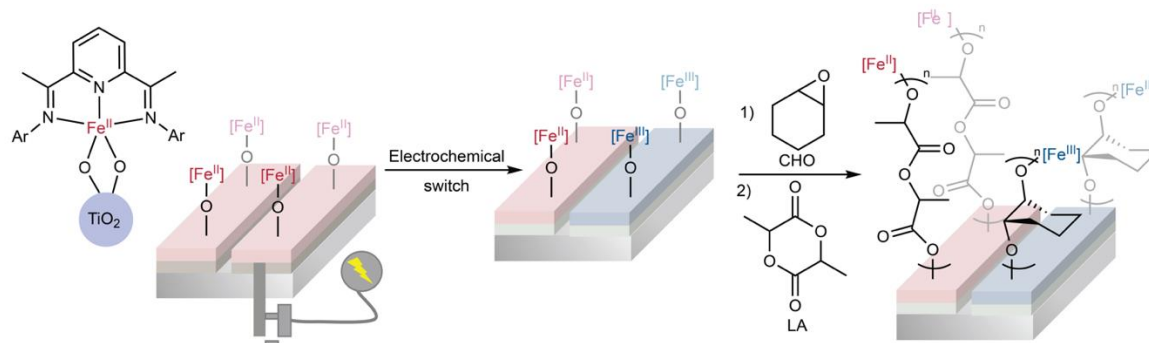
**a Host-guest system for hydrogenation of CO<sub>2</sub> to CH<sub>3</sub>OH**



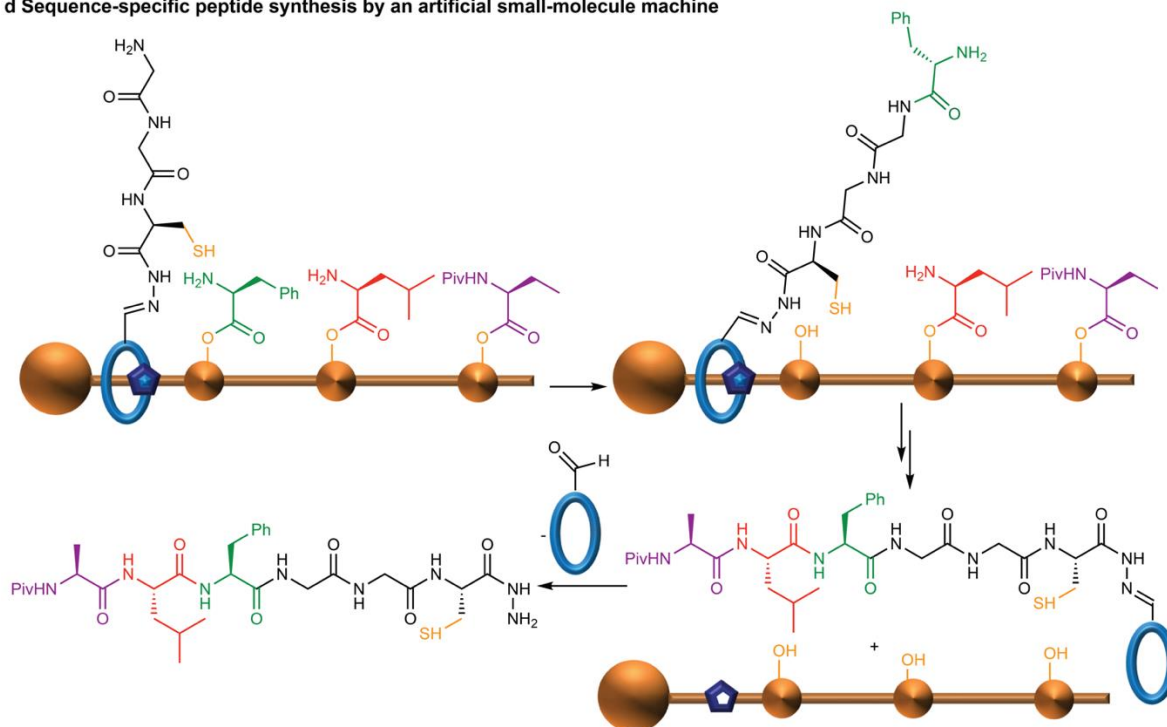
**b Catalytic cycle of incompatible steps by an [O<sub>2</sub>] gradient**



**c Patterning of surfaces using electrochemically switchable polymerization**



**d Sequence-specific peptide synthesis by an artificial small-molecule machine**



497

498 **Fig. 5] Applications of integrated catalysis.** a) Metal-organic framework (MOF) host-guest system for tandem CO<sub>2</sub>  
 499 hydrogenation to CH<sub>3</sub>OH via two separate ruthenium species encapsulated in a MOF (note: only one octahedral cage  
 500 of the MOFs is shown for simplicity). b) O<sub>2</sub> mediated CH<sub>4</sub> oxidation to CH<sub>3</sub>OH via an air sensitive Rh(II) intermediate

501 enabled in air by an electrochemically generated O<sub>2</sub> gradient. c| Integration of electrochemically catalyzed CO<sub>2</sub>  
502 reduction to CO and organometallic catalyzed ethylene/CO copolymerization for polyketone synthesis. d|  
503 Electrochemical control of a redox-switchable iron compound supported on a TiO<sub>2</sub> surface with two electronically  
504 isolated sections leading to different polymerization reactions. e| Sequence specific peptide synthesis by localizing  
505 the amino acid building blocks on a rotaxane.

506

## 507 [H1] Results

508 For temporal control, prior to reporting any catalytic results, it is essential to characterize the activity of  
509 the molecular catalyst in different states. NMR spectroscopy is the most commonly employed method for  
510 diamagnetic compounds, while other approaches like UV-vis spectroscopy can be used for paramagnetic  
511 compounds. When reporting the activity and selectivity of a catalyst in different states, vitality is  
512 important to rule out the possible interference coming from the external stimulus. Thus, control  
513 experiments should always be performed and reported. Furthermore, the addition and presence of a  
514 substrate in the reaction medium, i.e., from an incomplete reaction, may alter the nature of the  
515 catalytically active species and change its activity toward another substrate. Therefore, future research  
516 would benefit substantially from detailed experiment procedures, e.g., the concentrations and order of  
517 addition, when reactivity results are reported.

518 To confirm spatial control, one may employ a suite of characterization methods for heterogeneous  
519 systems. For example, in immobilizing a catalyst onto a surface, solid state NMR spectroscopy can help  
520 confirm and also determine the nature of a bound species.<sup>162</sup> Other methods such as FTIR spectroscopy  
521 can confirm the presence of key functional groups on the surface, while inductively coupled plasma -  
522 optical emission spectrometry (ICP-OES) can assess catalyst loading on the solid support.<sup>33</sup>

523 When combining two or more spatially controlled catalytic systems, mass transport between catalysts  
524 may understandably cloud reporting of reaction rates. In order to assess the extent to which mass  
525 transport alters observed reaction rates, the  $\Phi$  criterion proves useful.<sup>163,164</sup> Developed in the middle to  
526 late 1900s, the  $\Phi$  criterion can provide a qualitative assessment of mass transport. Derived from the  
527 reaction rate, concentration, diffusion coefficient of the species to be transported, and diffusion path  
528 length, if  $\Phi < 1$ , then one may ignore diffusional effects on reported reaction rates and kinetics. However,  
529 if  $\Phi > 1$ , one cannot ignore the effect of mass transport. In addition to providing insight into the interplay  
530 of mass transport and kinetics in integrated catalysis, the  $\Phi$  criterion can also provide a justification for  
531 exploring ways to alleviate mass transport (vide infra).

532

## 533 [H1] Applications

534 Integrated spatiotemporally controlled catalysis, although rare, has been employed to construct  
535 sophisticated systems and solve compatibility problems between multiple catalytic cycles. Such  
536 applications include small molecule activation, polymerization, and surface patterning. Although the  
537 development of integrated catalysis is still in its infancy, and some examples are not strictly, by definition,

538 an integrated system, they demonstrate the potential of integrated catalysis and how it can be exploited  
539 in synthesizing products with high complexity.

## 540 [H2] Confinement

541 Integrated catalysis can address thermodynamic constraints in sequences of chemical reactions. For  
542 example, the power of encapsulating transition metal catalysts in metal organic frameworks (MOFs) for  
543 integrated catalysis was recently demonstrated for the efficient hydrogenation of CO<sub>2</sub> to methanol.<sup>19,165</sup>  
544 In this example (FIG. 5a), two different ruthenium complexes were encapsulated in UiO-66, enabling a  
545 tandem catalytic reaction in three steps: the thermodynamically unfavorable hydrogenation of CO<sub>2</sub> to  
546 formic acid catalyzed by a PNP ruthenium complex; the near thermoneutral conversion of formic acid to  
547 formate ester catalyzed by the zirconium oxide nodes of UiO-66; the thermodynamically favored  
548 hydrogenation of formate ester to methanol catalyzed by a PNN ruthenium complex. This catalyst system  
549 overcomes the thermodynamic limitations associated with the hydrogenation of CO<sub>2</sub> to formic acid by  
550 coupling it with the thermodynamically favored hydrogenation of formate esters. If the first step was  
551 separated from the second two in a sequential process, no formic acid would be obtained. Importantly,  
552 no methanol was observed unless at least one of the two ruthenium-based complexes was encapsulated  
553 in UiO-66, and catalyst recyclability was only possible if both ruthenium complexes were encapsulated in  
554 UiO-66. These observations highlight the benefits of catalyst compartmentalization to prevent undesired  
555 catalyst-catalyst interactions.

## 556 [H2] Concentration gradients

557 Another form of spatial control that has been beneficial for integrated catalysis is the generation of local  
558 concentration gradients, which can be conveniently achieved electrochemically. Depending on the  
559 steepness of the gradient, areas rich or void of certain species may be loosely defined as compartments.  
560 For example, a nanowire-array electrode can be employed to reconcile incompatibility between CH<sub>4</sub>  
561 activation by an O<sub>2</sub>-sensitive rhodium(II) metalloradical with O<sub>2</sub>-based oxidation for CH<sub>3</sub>OH formation (FIG.  
562 5b).<sup>20,166</sup> A reducing potential applied to the nanowire array electrode generated an O<sub>2</sub> gradient along the  
563 wire, and an anoxic, essentially O<sub>2</sub> free zone was established at the bottom of the wires. As a result, an  
564 efficient catalytic cycle was established in which the air-sensitive Rh(II) activated CH<sub>4</sub> in the anoxic region,  
565 whereas CH<sub>3</sub>OH synthesis proceeded in the aerobic region with O<sub>2</sub> as the terminal oxidant. When a planar  
566 electrode was used, such a result was unattainable, showing that the O<sub>2</sub> gradient of the nanowire array  
567 was responsible for reconciling incompatibility. The effective detainment of the ephemeral Rh(II)  
568 intermediate by the nanowire electrode for catalytic CH<sub>4</sub>-to-CH<sub>3</sub>OH conversion<sup>20,166</sup> encourages further  
569 exploration in utilizing microscopic concentration gradients in catalysis to reconcile incompatibility.

570 A similar strategy using the electrochemical method to control the concentration of small molecules can  
571 also be applied in generating CO from CO<sub>2</sub> then utilizing the produced CO as a building block in subsequent  
572 reactions. Considering that CO<sub>2</sub> is abundant and is one of the culprits of climate change, deriving reactive  
573 building blocks from it and converting them into value-added products would be ideal and could benefit  
574 substantially from integrated catalysis. For example, CO produced from CO<sub>2</sub> was utilized as the carbon  
575 feedstock in reactions such as Fischer–Tropsch, hydroformylation, and carbonylation.<sup>167</sup> Furthermore, in

576 reactions like CO and ethylene copolymerization, the pressure of CO was fine-tuned electrochemically,  
577 and the amount of CO incorporated was modulated in an integrated catalytic system to control the  
578 structure of the resulting polyketone (FIG. 5c).<sup>168</sup>

## 579 [H2] Solid-state polymerization

580 Integrated catalysis can generate highly complex products, such as a precisely controlled macromolecular  
581 structure,<sup>58,59,169,170</sup> but the spatiotemporal control that is inherent to integrated catalysis has also been  
582 exploited to synthesize patterned polymer-functionalized surfaces (FIG. 5d).<sup>171</sup> By immobilizing redox-  
583 switchable bis(imino)pyridine iron polymerization catalyst to semiconducting TiO<sub>2</sub> nanoparticles, redox-  
584 switchable polymerization reactions can be carried out in the solid state. Suspending the iron(II)-  
585 functionalized TiO<sub>2</sub> nanoparticles on conducting fluorine-doped tin oxide surfaces led to electroactive  
586 surfaces whose chemoselectivity for polymerization can be altered through the application of an electrical  
587 current: surfaces with the catalyst in the iron(II) oxidation state react with lactide to form polyesters while  
588 surfaces that have been exposed to oxidizing potentials result in oxidation of the catalyst to the iron(III)  
589 oxidation state, which reacts with epoxides to form polyethers. By using fluorine-doped tin oxide  
590 substrates that contain electrically isolated zones of the functionalized TiO<sub>2</sub> nanoparticles, patterned  
591 surfaces containing polyesters and polyethers can be synthesized by applying oxidizing potentials to zones  
592 where polyethers are desired.

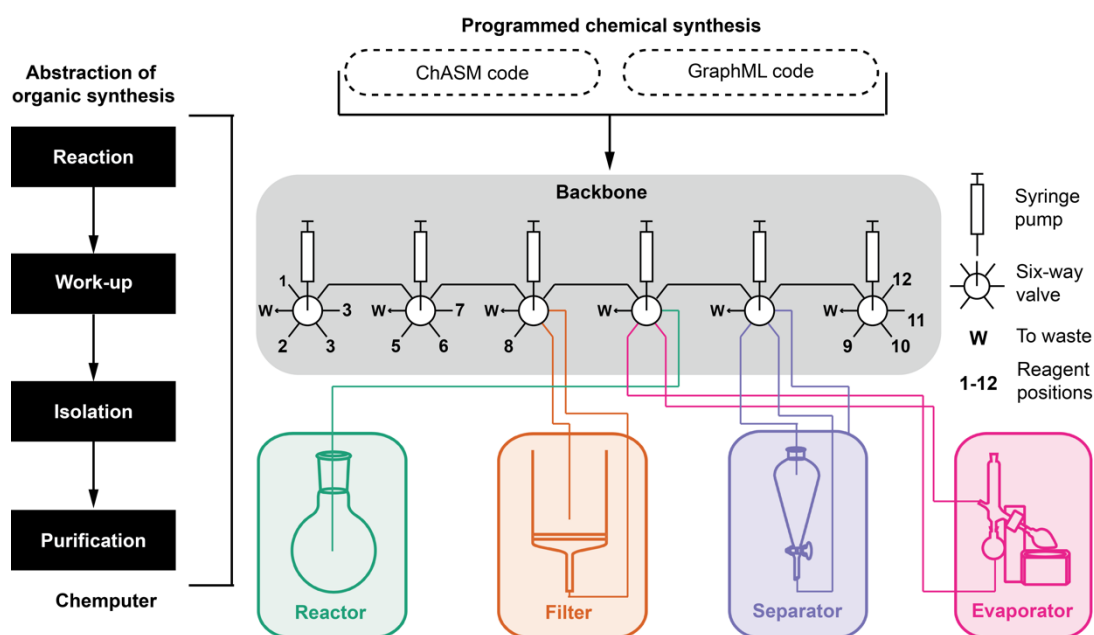
## 593 [H2] Molecular machines

594 Another example of synthesizing products of high complexity is the application of a molecular machine in  
595 peptide synthesis. An artificial molecular machine was developed to mimic nature's ribosome and  
596 synthesize oligopeptides with a predetermined sequence (FIG. 5e).<sup>170</sup> The system consists of a rotaxane,  
597 an axle with protected amino acids immobilized to it, and a bulky end-stopper. The rotaxane has a  
598 polypeptide arm that contains a cysteine moiety and a terminal glycyglycine amine group. The  
599 oligopeptide synthesis is accomplished by a series of O-S and S-N acyl transfers as the rotaxane moves  
600 along the axle. Though the system is only capable of incorporating up to 4 amino acids and is not catalytic,  
601 it still represents a valuable proof of concept that demonstrates how artificial synthesis can mimic nature.  
602 Furthermore, it illuminates an encouraging direction that, beyond stoichiometric templating, an  
603 integrated system, showing spatial and temporal control, may be able to deliver the synthesis of highly  
604 complex products.

## 605 [H2] Automation

606 Finally, the benefits of integrated catalysis are amenable to future automation strategies, such as the  
607 Chemputer. Like in biocatalysis, where high-throughput screening can help identify the best protein from  
608 the vast genome database among numerous candidates and myriad mutations, integrated catalysis could  
609 also benefit from a highly automated synthesis-characterization-analysis system when devising a complex  
610 system involving multiple catalytic cycles to optimize the working conditions, e.g., solvent, temperature,  
611 concentrations, and cocatalyst. Other than the well-established peptide and nucleotide syntheses,  
612 laboratory-scale synthesis of complicated products is still mainly performed manually. The Chemputer  
613 demonstrates an efficient automation of multistep synthesis and purification processes (FIG. 6).<sup>172</sup> By

614 using programming, various synthetic procedures can be abstracted from written protocols, translated  
 615 into machine language and implemented on synthetic modules to prepare pharmaceutical compounds.  
 616 The Chemputer may be as or more efficient than a traditional iterative lab approach, without any human  
 617 intervention. Furthermore, the Chemputer was specifically designed to be amenable to variations in the  
 618 sequence of steps performed, to allow adaptation to a wide array of chemical processes. In addition, such  
 619 a synthetic platform allows for the standardization of chemical synthesis, minimizing irreproducibility  
 620 caused by the synthetic nuances that are often omitted or assumed already known by the reader.<sup>172,173</sup>



621  
 622 Fig. 6 | Organic synthesis in a robotic system enabled by the application of a chemical programming language to an  
 623 automated synthetic set up.

624  
 625 **[H1] Reproducibility and data deposition**

626 **[H2] Reproducibility**

627 The degradation of catalysts during a reaction is one of the main problems in catalysis. Degradation has  
 628 an even more profound impact on switchable catalysis, as the switching process introduces additional  
 629 possible degradation pathways. Therefore, a judicious choice of the most compatible external stimulus  
 630 may be the key to successful switchable catalysis. In addition, for catalysts confined onto surfaces, mass  
 631 transfer may slow down the overall reaction rate and is influenced by the distance and diffusivity between  
 632 the two catalysts. While this property can be exploited for integrated catalysis (for example, capitalizing  
 633 on local concentration gradients), if the physical location or diffusivity of the catalysts is not well controlled  
 634 (stirring, solvent, temperature), irreproducible results can be problematic.

635 In addition to the chemical and engineering complications that exist with integrated catalysis, there also  
 636 is an analytical challenge to address when catalysts are spatially confined. For homogeneous catalytic  
 637 systems, the characterization methods are diverse and often diagnostic, such as NMR spectroscopy and

638 X-ray crystallography. However, when the catalyst is compartmentalized or immobilized on a solid surface,  
639 the system becomes complex, and characterization needs to involve relatively complicated techniques.  
640 Some spectroscopic methods such as X-ray photoelectron spectroscopy, inductively coupled plasma mass  
641 spectrometry (ICP-MS), and ICP-OES can be used to obtain elemental information either for the surface  
642 or the bulk powder. Infrared, Raman, absorption, and solid state NMR spectroscopy can facilitate  
643 understanding the nature of the active species. However, additional characterization methods are  
644 necessary for a detailed and precise chemical structure of the catalytic system that would ensure  
645 reproducibility. Especially in an integrated system, using operando techniques to understand the  
646 mechanism of the reaction and the interactions between catalyst-catalyst, catalyst-substrate, and  
647 substrate-substrate under working conditions will be extremely beneficial.<sup>174,175</sup>

## 648 **[H2] Database**

649 The field would benefit from a database of coupled tandem to use as a reference when constructing  
650 complicated integrated catalytic systems. When possible, the catalytic reactions involved, the  
651 spatiotemporal control methods and reaction conditions employed, and how the activity and selectivity  
652 of the overall reaction compared to the isolated stepwise reactions should be deposited. A database of  
653 the resulting products would also be informative. In the case of polymerization reactions, for example,  
654 many copolymers are synthesized using tandem polymerization reactions, and while there are databases  
655 listing the structures and properties of polymers, such as [PolyInfo](#), [Polymer Property Predictor and Database](#),  
656 and [CAMPUS](#), these databases are far from comprehensive in summarizing the structures and  
657 corresponding properties of the various copolymers produced and reported. If this information could be  
658 benchmarked and centralized, it could provide guidance for future polymer design and retrosynthesis.

## 659 **[H1] Limitations and optimizations**

660 A major limitation of the current state of iterative chemical synthesis is inefficiencies related to time and  
661 material involved in workup steps, which may also lead to decreased yields.<sup>176</sup> An integrated catalytic  
662 approach can alleviate this drawback, as well as pave the way to obtaining complex products from simple  
663 feedstocks. As a field that continues to evolve, integrated catalysis still faces many challenges. First is the  
664 issue of compatibility. Compatibility considerations in integrated systems is multifaceted and includes the  
665 compatibility between catalysts, reagents, solvents and reaction conditions. When different reaction  
666 cycles are carried out in one pot, the catalysts may undergo deactivation or decomposition caused by the  
667 substrates or cocatalysts of another reaction. In principle, switchable catalysis circumvents the problem  
668 by generating different catalytic species at different times, while spatial control can be used to separate  
669 different precatalysts. Furthermore, when different reactions require different conditions, such as  
670 temperature and pressure, reconciling such disparity is pivotal. Again, spatial control becomes important  
671 by separating such reactions in different microenvironments (such as compartmentalization,  
672 immobilization, or electrochemically generated concentration gradients).

673 Limitations and potential drawbacks may be related to the temporal control of a catalyst. For example,  
674 the mode of temporal control (photochemical, electrochemical, or chemical) may not be compatible with  
675 other reagents in the reaction medium. An applied potential or light source that switches a catalyst

676 between active states may have undesired consequences on other species in solution. One method to  
677 circumvent this incompatibility would be to spatially separate the species of interest. For example, if a  
678 catalyst is to be switched electrochemically, immobilizing it onto the electrode surface may help prevent  
679 some unwanted redox reactions with other species. However, if the other species are free to diffuse, they  
680 may still be decomposed by an applied potential. Further, compartmentalization of the incompatible  
681 species could also help. Thus, great care must be taken to ensure other species in an integrated system  
682 are compatible with the means of temporal control.

683 With respect to spatially localizing a catalyst, mass transport can become important. The heterogenization  
684 of a previously homogeneous catalyst introduces transport from the bulk solution to the catalyst site as a  
685 fundamental step for catalysis to proceed. Should this step prove limiting, it may be counterproductive to  
686 spatially control a catalyst. Instead of relying solely on diffusion, the introduction of fluid transport may  
687 help overcome mass transport limitations.<sup>177-181</sup> Further, conducting a reaction in flow provides numerous  
688 additional parameters, such as flow rate and residence time, providing more opportunities for  
689 optimization compared to a batch process. Mass transport limitations may also be exploited to avoid  
690 unwanted background reactions. This would greatly depend on the pervasiveness of such mass transport  
691 limitations, as well as the competition between diffusive and kinetic phenomena.<sup>164</sup>

692 When employing spatiotemporal control to build an integrated catalytic system, one must take into  
693 account some key considerations. The compatibility and practicality of all components of an integrated  
694 system should be considered. First, all possible combinations of controls should be tested to assess  
695 compatibility between catalysts, catalysts and reactants, and reactants. Simple outputs such as percent  
696 conversion can be used to assess the effect of one reagent on another with respect to maintaining or  
697 diminishing activity. In addition, assuming the separate catalyst systems have different optimal conditions  
698 (such as temperature, solvent, pressure) compatible middle ground conditions must be determined. In  
699 the event there is an incompatibility between some reagents in the two systems, spatial and/or temporal  
700 control may be implemented to circumvent the mutual deactivation.

701 For spatial control, a key consideration is whether the catalyst/reagents need to be separated or can  
702 feasibly be immobilized onto a surface or confined within an easily accessible compartment. For temporal  
703 control, when incorporating switchable catalysis to either achieve on/off control or to open more avenues  
704 for different reactions, electronic effect of a redox catalyst, the ring opening/closing of a photochromic  
705 moiety, or the metal cation coordination onto a pendant ligand can be used, depending on the reaction  
706 conditions. For example, if the reagents/substrates/products in the system are colored, then it might be  
707 easier to add a redox-switchable or metal cation coordinating moiety to the ligand framework to realize  
708 a switch in catalytic activity rather than employing light as the external stimulus. On the other hand, if  
709 switchable catalysis requires intercepting short-lived reactive intermediates, then light may be the most  
710 appropriate external stimulus to target. The next thing to consider is whether the exogenous trigger  
711 interferes with the catalytic transformation itself. If the system is non-colored and remote control is  
712 preferred, then a photoswitch or an electrochemical switch are the most viable options as neither  
713 technique requires adding reagents to the reaction. Finally, practicality is as equal if not the most  
714 important consideration. The most intricate spatial and temporal methods may be developed and applied

715 to address any conceivable compatibility issues. However, the time and effort spent should not be greater  
716 than that of the combined systems treated independently. Thus, researchers must critically evaluate and  
717 determine what compatibility issues need to be addressed before considering what spatial and/or  
718 temporal methods to use and whether an integrated approach is superior to an approach involving  
719 sequential catalytic reactions.

## 720 **[H1] Outlook**

721 In integrated catalysis, different reactions are coupled in a single vessel to generate products with high  
722 complexity from a mixture of abundant starting materials. Inspired by macromolecule synthesis in living  
723 cells, artificial catalysis for the synthesis of polymers with a well-defined sequence and microstructure has  
724 been achieved in one pot with the proper utilization of integrated spatial and temporal control. Biological  
725 macromolecules, such as proteins and DNA, encode information in their sequences and structures.  
726 Likewise, the sequence and structure of synthetic macromolecules dictate their properties. We envisage  
727 that integrated catalysis can become the machinery for synthesizing novel molecules and materials with  
728 distinct properties. In addition to macromolecules, integrated catalysis can also be an effective tool for  
729 multistep syntheses, and asymmetric syntheses of organic small molecules, such as pharmaceuticals.

730 Careful design of catalyst combinations in tandem catalytic cycles may enable reactions to proceed under  
731 mild conditions and improve the selectivity and yield of the overall process. More importantly, integrated  
732 catalysis can capture unstable, transient, and hazardous intermediates,<sup>182-184</sup> and subsequently convert  
733 them into stable and valuable products, thus expanding synthetic capabilities. For example, by coupling  
734 an exothermic and endothermic reaction, thermodynamic leveraging in tandem reactions can drive the  
735 formation of otherwise unviable products.<sup>19,165,185,186</sup> Furthermore, breaking down a thermodynamically  
736 favorable but high activation energy reaction into a series of steps that can be optimized individually, can  
737 lower the overall energy barrier and allow the reaction to proceed through milder conditions.

738 To achieve precisely controlled and widely applicable integrated catalytic systems, it is imperative to  
739 enrich and update the toolbox available by adding emerging methods for spatial and temporal control. As  
740 a complement to artificial catalysis, biocatalysis is also indispensable, and often provides exquisite  
741 selectivity. Thus, the construction of hybrid catalyst systems that involve biocatalysis and artificial spatial-  
742 temporally controlled catalysis is an exciting new direction for integrated catalysis.<sup>145</sup> Finally, when  
743 implementing integrated catalysis, engineering aspects such as reactor design are also crucial to ensure  
744 that the anticipated results can be achieved.

745 Another way to facilitate the design of integrated catalytic systems is to use simulations and predictions  
746 that evaluate structure-activity-selectivity relationships to identify the best catalyst in a timely manner.  
747 Recent advances in quantum mechanical and finite element simulations now make possible an holistic  
748 analysis of the entire integrated system that takes into account all contributing factors.<sup>187</sup> In this regard,  
749 screening of catalysts for isolated reactions should be coupled with first-principles calculations and data  
750 science to optimize the integrated system. Computer-assisted calculations can also be used in conjunction  
751 with high-throughput automation<sup>188</sup> to further expedite screening and streamline the synthetic routes to  
752 achieve high efficiency, low waste, and low cost.

753 **Glossary**

754 **Cascade / Domino process:** A transformation that installs two or more bonds under identical conditions  
755 and with the same mechanism.

756  
757 **Chemswitchable catalysis:** A reaction in which the selectivity of a catalyst can be reversibly altered by  
758 a chemical trigger.

759  
760 **Compartmentalization:** Spatial localization of one or multiple species within a well-defined  
761 encapsulation or confinement, where entry and exit within the compartment is dependent on the  
762 chemical makeup of both the compartment and diffusing species.

763  
764 **Orthogonal reactivity:** Reactivity of a multistate catalyst toward different substrates: catalyst is active in  
765 one state for one type of reaction and inactive for another, and shows the opposite trend in the other  
766 state.

767  
768 **Redox-switchable catalysis:** The reactivity or selectivity of a catalyst that can be reversibly altered by  
769 changing its oxidation state.

770  
771 **Ring opening polymerization:** A chain growth polymerization reaction in which the polymer chain  
772 propagation is achieved by the reactive terminus attacking and ring opening a cyclic monomer to  
773 elongate the polymer chain and generate a new active terminus.

774  
775 **Surface immobilization:** Spatial localization of a typically homogeneous species onto a heterogeneous  
776 support.

777  
778 **Tandem process:** Coupled catalytic processes in which substrates are converted sequentially by two or  
779 more mechanistically distinct reactions.

## 780 References

- 781 1 Kätelhön, A., Meys, R., Deutz, S., Suh, S. & Bardow, A. Climate change mitigation  
782 potential of carbon capture and utilization in the chemical industry. *Proc. Natl. Acad. Sci.*  
783 *USA* **116**, 11187-11194, doi:10.1073/pnas.1821029116 (2019).
- 784 2 Agency, I. E. Tracking clean energy progress 2017. *Energy Technol. Perspect 2017* (2017).
- 785 3 Zweifel, G. S., Nantz, M. H. & Somfai, P. *Modern organic synthesis: an introduction*.  
786 (John Wiley & Sons, 2017).
- 787 4 Lohr, T. L. & Marks, T. J. Orthogonal tandem catalysis. *Nat. Chem.* **7**, 477-482,  
788 doi:10.1038/nchem.2262 (2015).
- 789 5 Wasilke, J.-C., Obrey, S. J., Baker, R. T. & Bazan, G. C. Concurrent tandem catalysis.  
790 *Chem. Rev.* **105**, 1001-1020, doi:10.1021/cr020018n (2005).
- 791 6 Goldman, A. S. Catalytic alkane metathesis by tandem alkane dehydrogenation-olefin  
792 metathesis. *Science* **312**, 257-261, doi:10.1126/science.1123787 (2006).
- 793 7 Leitch, D. C., Lam, Y. C., Labinger, J. A. & Bercaw, J. E. Upgrading light hydrocarbons via  
794 tandem catalysis: a dual homogeneous Ta/Ir system for alkane/alkene coupling. *J. Am.*  
795 *Chem. Soc.* **135**, 10302-10305, doi:10.1021/ja405191a (2013).
- 796 8 Lu, J., Dimroth, J. & Weck, M. Compartmentalization of incompatible catalytic  
797 transformations for tandem catalysis. *J. Am. Chem. Soc.* **137**, 12984-12989,  
798 doi:10.1021/jacs.5b07257 (2015).
- 799 9 Xie, C. *et al.* Tandem catalysis for CO<sub>2</sub> hydrogenation to C<sub>2</sub>-C<sub>4</sub> hydrocarbons. *Nano Lett.*  
800 **17**, 3798-3802, doi:10.1021/acs.nanolett.7b01139 (2017).
- 801 10 Cho, H. J., Kim, D., Li, J., Su, D. & Xu, B. Zeolite-encapsulated Pt nanoparticles for tandem  
802 catalysis. *J. Am. Chem. Soc.* **140**, 13514-13520, doi:10.1021/jacs.8b09568 (2018).
- 803 11 Wei, W., Wu, S., Shen, X., Zhu, M. & Li, S. Nanoreactor with core-shell architectures used  
804 as spatiotemporal compartments for "undisturbed" tandem catalysis. *J. Inorg.*  
805 *Organomet. Polym. Mater.* **29**, 1235-1242, doi:10.1007/s10904-019-01087-2 (2019).
- 806 12 Song, Y. *et al.* Multistep engineering of synergistic catalysts in a metal-organic  
807 framework for tandem C-O bond cleavage. *J. Am. Chem. Soc.* **142**, 4872-4882,  
808 doi:10.1021/jacs.0c00073 (2020).
- 809 13 Qu, P., Kuepfert, M., Hashmi, M. & Weck, M. Compartmentalization and  
810 photoregulating pathways for incompatible tandem catalysis. *J. Am. Chem. Soc.* **143**,  
811 4705-4713, doi:10.1021/jacs.1c00257 (2021).
- 812 14 Shyshkanov, S., Vasilyev, D. V., Abhyankar, K. A., Stylianou, K. C. & Dyson, P. J. Tandem  
813 Pauson-Khand reaction using carbon dioxide as the C<sub>1</sub>-source. *Eur. J. Inorg. Chem.* **2022**,  
814 doi:10.1002/ejic.202200037 (2022).
- 815 15 Schmidt, S., Castiglione, K. & Kourist, R. Overcoming the incompatibility challenge in  
816 chemoenzymatic and multi-catalytic cascade reactions. *Chem. A Eur. J.* **24**, 1755-1768,  
817 doi:10.1002/chem.201703353 (2018).
- 818 16 Meng, J. *et al.* Switchable catalysts used to control Suzuki cross-coupling and aza-  
819 Michael addition/asymmetric transfer hydrogenation cascade reactions. *ACS Catal.* **9**,  
820 8693-8701, doi:10.1021/acscatal.9b01593 (2019).

821 17 Matthey, A. P. *et al.* Development of continuous flow systems to access secondary  
822 amines through previously incompatible biocatalytic cascades. *Angew. Chem. Int. Ed.* **60**,  
823 18660-18665, doi:10.1002/anie.202103805 (2021).

824 18 Natinsky, B. S., Jolly, B. J., Dumas, D. M. & Liu, C. Efficacy analysis of  
825 compartmentalization for ambient CH<sub>4</sub> activation mediated by a Rh<sup>II</sup> metalloradical in a  
826 nanowire array electrode. *Chem. Sci.* **12**, 1818-1825, doi:10.1039/d0sc05700b (2021).

827 19 Rayder, T. M., Bensalah, A. T., Li, B., Byers, J. A. & Tsung, C.-K. Engineering second  
828 sphere interactions in a host–guest multicomponent catalyst system for the  
829 hydrogenation of carbon dioxide to methanol. *J. Am. Chem. Soc.* **143**, 1630-1640,  
830 doi:10.1021/jacs.0c08957 (2021).

831 20 Natinsky, B. S., Lu, S., Copeland, E. D., Quintana, J. C. & Liu, C. Solution catalytic cycle of  
832 incompatible steps for ambient air oxidation of methane to methanol. *ACS Cent. Sci.* **5**,  
833 1584-1590, doi:10.1021/acscentsci.9b00625 (2019).

834 21 Hurlley, S. Location, location, location. *Science* **326**, 1205-1205,  
835 doi:10.1126/science.326.5957.1205 (2009).

836 22 Chen, A. H. & Silver, P. A. Designing biological compartmentalization. *Trends Cell Biol.*  
837 **22**, 662-670, doi:10.1016/j.tcb.2012.07.002 (2012).

838 23 Leenders, S. H. A. M., Gramage-Doria, R., De Bruin, B. & Reek, J. N. H. Transition metal  
839 catalysis in confined spaces. *Chem. Soc. Rev.* **44**, 433-448, doi:10.1039/c4cs00192c  
840 (2015).

841 24 KÜchler, A., Yoshimoto, M., Luginbühl, S., Mavelli, F. & Walde, P. Enzymatic reactions in  
842 confined environments. *Nat. Nanotechnol.* **11**, 409-420, doi:10.1038/nnano.2016.54  
843 (2016).

844 25 Tsitkov, S. & Hess, H. Design principles for a compartmentalized enzyme cascade  
845 reaction. *ACS Catal.* **9**, 2432-2439, doi:10.1021/acscatal.8b04419 (2019).

846 26 Vázquez-González, M., Wang, C. & Willner, I. Biocatalytic cascades operating on  
847 macromolecular scaffolds and in confined environments. *Nat. Catal.* **3**, 256-273,  
848 doi:10.1038/s41929-020-0433-1 (2020).

849 27 Jolly, B. J., Co, N. H., Davis, A. R., Diaconescu, P. L. & Liu, C. A generalized kinetic model  
850 for compartmentalization of organometallic catalysis. *Chem. Sci.* **13**, 1101-1110,  
851 doi:10.1039/D1SC04983F (2022).

852 28 Corma, A. & Garcia, H. Silica-bound homogenous catalysts as recoverable and reusable  
853 catalysts in organic synthesis. *ACS Catal.* **348**, 1391-1412, doi:10.1002/adsc.200606192  
854 (2006).

855 29 McCreery, R. L. Advanced carbon electrode materials for molecular electrochemistry.  
856 *Chem. Rev.* **108**, 2646-2687, doi:10.1021/cr068076m (2008).

857 30 Queffelec, C., Petit, M., Janvier, P., Knight, D. A. & Bujoli, B. Surface modification using  
858 phosphonic acids and esters. *Chem. Rev.* **112**, 3777-3807, doi:10.1021/cr2004212  
859 (2012).

860 31 Blakemore, J. D., Gupta, A., Warren, J. J., Brunschwig, B. S. & Gray, H. B. Noncovalent  
861 immobilization of electrocatalysts on carbon electrodes for fuel production. *J. Am.*  
862 *Chem. Soc.* **135**, 18288-18291, doi:10.1021/ja4099609 (2013).

- 863 32 Pujari, S. P., Scheres, L., Marcelis, A. T. & Zuilhof, H. Covalent surface modification of  
864 oxide surfaces. *Angew. Chem. Int. Ed.* **53**, 6322-6356, doi:10.1002/anie.201306709  
865 (2014).
- 866 33 Copéret, C. *et al.* Surface organometallic and coordination chemistry toward single-site  
867 heterogeneous catalysts: strategies, methods, structures, and activities. *Chem. Rev.* **116**,  
868 323-421, doi:10.1021/acs.chemrev.5b00373 (2016).
- 869 34 Wang, L., Polyansky, D. E. & Concepcion, J. J. Self-assembled bilayers as an anchoring  
870 strategy: catalysts, chromophores, and chromophore-catalyst assemblies. *J. Am. Chem.*  
871 *Soc.* **141**, 8020-8024, doi:10.1021/jacs.9b01044 (2019).
- 872 35 Wu, L. *et al.* Stable molecular surface modification of nanostructured, mesoporous  
873 metal oxide photoanodes by silane and click chemistry. *ACS Appl. Mater. Interfaces* **11**,  
874 4560-4567, doi:10.1021/acsami.8b17824 (2019).
- 875 36 Lu, S., Guan, X. & Liu, C. Electricity-powered artificial root nodule. *Nat. Commun.* **11**,  
876 doi:10.1038/s41467-020-15314-9 (2020).
- 877 37 Chen, Y., Wang, J., Hoar, B. B., Lu, S. & Liu, C. Machine learning–based inverse design for  
878 electrochemically controlled microscopic gradients of O<sub>2</sub> and H<sub>2</sub>O<sub>2</sub>. *Proc. Natl. Acad. Sci.*  
879 **119**, e2206321119, doi:doi:10.1073/pnas.2206321119 (2022).
- 880 38 Blanco, V., Leigh, D. A. & Marcos, V. Artificial switchable catalysts. *Chem. Soc. Rev.* **44**,  
881 5341-5370, doi:10.1039/c5cs00096c (2015).
- 882 39 Leibfarth, F. A., Mattson, K. M., Fors, B. P., Collins, H. A. & Hawker, C. J. External  
883 regulation of controlled polymerizations. *Angew. Chem. Int. Ed.* **52**, 199-210,  
884 doi:10.1002/anie.201206476 (2013).
- 885 40 Doerr, A. M. *et al.* Advances in polymerizations modulated by external stimuli. *ACS*  
886 *Catal.* **10**, 14457-14515, doi:10.1021/acscatal.0c03802 (2020).
- 887 41 Kaler, S. & Jones, M. D. Recent advances in externally controlled ring-opening  
888 polymerisations. *Dalton Trans.* **51**, 1241-1256, doi:10.1039/d1dt03471e (2022).
- 889 42 Teator, A. J., Lastovickova, D. N. & Bielawski, C. W. Switchable polymerization catalysts.  
890 *Chem. Rev.* **116**, 1969-1992, doi:10.1021/acs.chemrev.5b00426 (2016).
- 891 43 Choudhury, J. Recent developments on artificial switchable catalysis. *Tetrahedron Lett.*  
892 **59**, 487-495, doi:10.1016/j.tetlet.2017.12.070 (2018).
- 893 44 Lastovickova, D. N., Shao, H. L., Lu, G., Liu, P. & Bielawski, C. W. A ring-opening  
894 metathesis polymerization catalyst that exhibits redox-switchable monomer  
895 selectivities. *Chem. A Eur. J.* **23**, 5994-6000, doi:10.1002/chem.201605738 (2017).
- 896 45 Zou, W. P., Pang, W. M. & Chen, C. L. Redox control in palladium catalyzed norbornene  
897 and alkyne polymerization. *Inorg. Chem. Front.* **4**, 795-800, doi:10.1039/c6qi00562d  
898 (2017).
- 899 46 Anderson, W. C., Rhinehart, J. L., Tennyson, A. G. & Long, B. K. Redox-active ligands: an  
900 advanced tool to modulate polyethylene microstructure. *J. Am. Chem. Soc.* **138**, 774-  
901 777, doi:10.1021/jacs.5b12322 (2016).
- 902 47 Lorkovic, I. M., Duff, R. R. & Wrighton, M. S. Use of the redox-active ligand 1, 1'-bis  
903 (diphenylphosphino) cobaltocene to reversibly alter the rate of the rhodium (I)-  
904 catalyzed reduction and isomerization of ketones and alkenes. *J. Am. Chem. Soc.* **117**,  
905 3617-3618, doi:10.1021/ja00117a033 (1995).

906 48 Gregson, C. K. A. *et al.* Redox control within single-site polymerization catalysts. *J. Am.*  
907 *Chem. Soc.* **128**, 7410-7411, doi:10.1021/ja061398n (2006).

908 49 Zhao, M. H. & Chen, C. L. Accessing multiple catalytically active states in redox-  
909 controlled olefin polymerization. *ACS Catal.* **7**, 7490-7494, doi:10.1021/acscatal.7b02564  
910 (2017).

911 50 Varnado, C. D., Rosen, E. L., Collins, M. S., Lynch, V. M. & Bielawski, C. W. Synthesis and  
912 study of olefin metathesis catalysts supported by redox-switchable diaminocarbene [3]  
913 ferrocenophanes. *Dalton Trans.* **42**, 13251-13264, doi:10.1039/c3dt51278a (2013).

914 51 Doerr, A. M., Burroughs, J. M., Legaux, N. M. & Long, B. K. Redox-switchable ring-  
915 opening polymerization by tridentate ONN-type titanium and zirconium catalysts. *Catal.*  
916 *Sci. Technol.* **10**, 6501-6510, doi:10.1039/d0cy00642d (2020).

917 52 Anderson, W. C., Park, S. H., Brown, L. A., Kaiser, J. M. & Long, B. K. Accessing multiple  
918 polyethylene grades via a single redox-active olefin polymerization catalyst. *Inorg.*  
919 *Chem. Front.* **4**, 1108-1112, doi:10.1039/c7qi00079k (2017).

920 53 Brown, L. A., Rhinehart, J. L. & Long, B. K. Effects of ferrocenyl proximity and monomer  
921 presence during oxidation for the redox-switchable polymerization of l-lactide. *ACS*  
922 *Catal.* **5**, 6057-6060, doi:10.1021/acscatal.5b01434 (2015).

923 54 Wei, J. N. & Diaconescu, P. L. Redox-switchable ring-opening polymerization with  
924 ferrocene derivatives. *Acc. Chem. Res.* **52**, 415-424, doi:10.1021/acs.accounts.8b00523  
925 (2019).

926 55 Broderick, E. M. *et al.* Redox control of a ring-opening polymerization catalyst. *J. Am.*  
927 *Chem. Soc.* **133**, 9278-9281, doi:10.1021/ja2036089 (2011).

928 56 Broderick, E. M. & Diaconescu, P. L. Cerium(IV) catalysts for the ring-opening  
929 polymerization of lactide. *Inorg. Chem.* **48**, 4701-4706, doi:10.1021/ic802047u (2009).

930 57 Biernesser, A. B., Li, B. & Byers, J. A. Redox-controlled polymerization of lactide  
931 catalyzed by bis(imino)pyridine iron bis(alkoxide) complexes. *J. Am. Chem. Soc.* **135**,  
932 16553-16560, doi:10.1021/ja407920d (2013).

933 58 Qi, M., Dong, Q., Wang, D. & Byers, J. A. Electrochemically switchable ring-opening  
934 polymerization of lactide and cyclohexene oxide. *J. Am. Chem. Soc.* **140**, 5686-5690,  
935 doi:10.1021/jacs.8b02171 (2018).

936 59 Hern, Z. C. *et al.* ABC and ABAB block copolymers by electrochemically controlled ring-  
937 opening polymerization. *J. Am. Chem. Soc.* **143**, 19802-19808, doi:10.1021/jacs.1c08648  
938 (2021).

939 60 Quan, S. M., Wang, X., Zhang, R. & Diaconescu, P. L. Redox switchable copolymerization  
940 of cyclic esters and epoxides by a zirconium complex. *Macromolecules* **49**, 6768-6778,  
941 doi:10.1021/acs.macromol.6b00997 (2016).

942 61 Wei, J. N., Riffel, M. N. & Diaconescu, P. L. Redox control of aluminum ring-opening  
943 polymerization: A combined experimental and DFT investigation. *Macromolecules* **50**,  
944 1847-1861, doi:10.1021/acs.macromol.6b02402 (2017).

945 62 Xu, X., Luo, G., Hou, Z., Diaconescu, P. L. & Luo, Y. Theoretical insight into the redox-  
946 switchable activity of group 4 metal complexes for the ring-opening polymerization of  $\epsilon$ -  
947 caprolactone. *Inorg. Chem. Front.* **7**, 961-971 (2020).

948 63 Biernesser, A. B., Chiaie, K. R., Curley, J. B. & Byers, J. A. Block copolymerization of  
949 lactide and an epoxide facilitated by a redox switchable iron-based catalyst. *Angew.*  
950 *Chem. Int. Ed.* **55**, 5251-5254, doi:10.1002/anie.201511793 (2016).

951 64 Lai, A., Hern, Z. C. & Diaconescu, P. L. Switchable Ring-Opening Polymerization by a  
952 Ferrocene Supported Aluminum Complex. *ChemCatChem* **11**, 4210-4218,  
953 doi:10.1002/cctc.201900747 (2019).

954 65 Wang, X. *et al.* Redox Control of Group 4 Metal Ring-Opening Polymerization Activity  
955 toward L-Lactide and  $\epsilon$ -Caprolactone. *J. Am. Chem. Soc.* **136**, 11264-11267,  
956 doi:10.1021/ja505883u (2014).

957 66 Abubekеров, M. *et al.* Exploring oxidation state-dependent selectivity in polymerization  
958 of cyclic esters and carbonates with zinc (II) complexes. *iScience* **7**, 120-131,  
959 doi:10.1016/j.isci.2018.08.020 (2018).

960 67 Lowe, M. Y., Shu, S. S., Quan, S. M. & Diaconescu, P. L. Investigation of redox switchable  
961 titanium and zirconium catalysts for the ring opening polymerization of cyclic esters and  
962 epoxides. *Inorg. Chem. Front.* **4**, 1798-1805, doi:10.1039/c7qi00227k (2017).

963 68 Deng, S. & Diaconescu, P. L. A switchable dimeric yttrium complex and its three catalytic  
964 states in ring opening polymerization. *Inorg. Chem. Front.* **8**, 2088-2096,  
965 doi:10.1039/D0QI01479F (2021).

966 69 Ortuno, M. A. *et al.* The role of alkoxide initiator, spin state, and oxidation state in ring-  
967 opening polymerization of epsilon-caprolactone catalyzed by iron bis(imino)pyridine  
968 complexes. *Inorg. Chem.* **57**, 2064-2071, doi:10.1021/acs.inorgchem.7b02964 (2018).

969 70 Yoon, H. J., Kuwabara, J., Kim, J. H. & Mirkin, C. A. Allosteric supramolecular triple-layer  
970 catalysts. *Science* **330**, 66-69, doi:10.1126/science.1193928 (2010).

971 71 Kita, M. R. & Miller, A. J. M. Cation-modulated reactivity of iridium hydride pincer-crown  
972 ether complexes. *J. Am. Chem. Soc.* **136**, 14519-14529, doi:10.1021/ja507324s (2014).

973 72 Kita, M. R. & Miller, A. J. M. An ion-responsive pincer-crown ether catalyst system for  
974 rapid and switchable olefin isomerization. *Angew. Chem. Int. Ed.* **56**, 5498-5502,  
975 doi:10.1002/anie.201701006 (2017).

976 73 Camp, A. M. *et al.* Selecting double bond positions with a single cation-responsive  
977 iridium olefin isomerization catalyst. *J. Am. Chem. Soc.* **143**, 2792-2800,  
978 doi:10.1021/jacs.0c11601 (2021).

979 74 Cai, Z. Z., Xiao, D. W. & Do, L. H. Fine-tuning nickel phenoxyimine olefin polymerization  
980 catalysts: performance boosting by alkali cations. *J. Am. Chem. Soc.* **137**, 15501-15510,  
981 doi:10.1021/jacs.5b10351 (2015).

982 75 Cai, Z. Z. & Do, L. H. Thermally robust heterobimetallic palladium-alkali catalysts for  
983 ethylene and alkyl acrylate copolymerization. *Organometallics* **37**, 3874-3882,  
984 doi:10.1021/acs.organomet.8b00561 (2018).

985 76 Tran, T. V., Karas, L. J., Wu, J. I. & Do, L. H. Elucidating secondary metal cation effects on  
986 nickel olefin polymerization catalysts. *ACS Catal.* **10**, 10760-10772,  
987 doi:10.1021/acscatal.0c02949 (2020).

988 77 Tran, T. V., Nguyen, Y. H. & Do, L. H. Development of highly productive nickel-sodium  
989 phenoxyphosphine ethylene polymerization catalysts and their reaction temperature  
990 profiles. *Polym. Chem.* **10**, 3718-3721, doi:10.1039/c9py00610a (2019).

- 991 78 Tran, T. V., Lee, E., Nguyen, Y. H., Nguyen, H. D. & Do, L. H. Customizing polymers by  
992 controlling cation switching dynamics in non-living polymerization. *J. Am. Chem. Soc.*  
993 **144**, 17129-17139, doi:10.1021/jacs.2c07098 (2022).
- 994 79 Romain, C. & Williams, C. K. Chemoselective polymerization control: from mixed-  
995 monomer feedstock to copolymers. *Angew. Chem. Int. Ed.* **53**, 1607-1610,  
996 doi:10.1002/anie.201309575 (2014).
- 997 80 Coulembier, O., Moins, S., Todd, R. & Dubois, P. External and reversible CO<sub>2</sub> regulation  
998 of ring-opening polymerizations based on a primary alcohol propagating Species.  
999 *Macromolecules* **47**, 486-491, doi:10.1021/ma4024944 (2014).
- 1000 81 Lv, C. N., He, C. Z. & Pan, X. C. Oxygen-initiated and regulated controlled radical  
1001 polymerization under ambient conditions. *Angew. Chem. Int. Ed.* **57**, 9430-9433,  
1002 doi:10.1002/anie.201805212 (2018).
- 1003 82 Zhang, B. H. *et al.* Enzyme-initiated reversible addition-fragmentation chain transfer  
1004 polymerization. *Macromolecules* **48**, 7792-7802, doi:10.1021/acs.macromol.5b01893  
1005 (2015).
- 1006 83 Sha, S.-C. *et al.* Cation- $\pi$  interactions in the benzylic arylation of toluenes with bimetallic  
1007 catalysts. *J. Am. Chem. Soc.* **140**, 12415-12423, doi:10.1021/jacs.8b05143 (2018).
- 1008 84 Neilson, B. M. & Bielawski, C. W. Illuminating photoswitchable catalysis. *ACS Catal.* **3**,  
1009 1874-1885, doi:10.1021/cs4003673 (2013).
- 1010 85 Dorel, R. & Feringa, B. Photoswitchable catalysis based on the isomerisation of double  
1011 bonds. *Chem. Commun.* **55**, 6477-6486, doi:10.1039/c9cc01891c (2019).
- 1012 86 Wurthner, F. & Rebek, J. Light-switchable catalysis in synthetic receptors. *Angew. Chem.*  
1013 *Int. Ed.* **34**, 446-448, doi:10.1002/anie.199504461 (1995).
- 1014 87 Fu, C. K., Xu, J. T. & Boyer, C. Photoacid-mediated ring opening polymerization driven by  
1015 visible light. *Chem. Commun.* **52**, 7126-7129, doi:10.1039/c6cc03084j (2016).
- 1016 88 Berkovic, G., Krongauz, V. & Weiss, V. Spiropyran and spirooxazines for memories and  
1017 switches. *Chem. Rev.* **100**, 1741-1753, doi:10.1021/cr9800715 (2000).
- 1018 89 Majee, D. & Presolski, S. Dithienylethene-based photoswitchable catalysts: state of the  
1019 art and future perspectives. *ACS Catal.* **11**, 2244-2252, doi:10.1021/acscatal.0c05232  
1020 (2021).
- 1021 90 Eisenreich, F. *et al.* A photoswitchable catalyst system for remote-controlled  
1022 (co)polymerization in situ. *Nat. Catal.* **1**, 516-522, doi:10.1038/s41929-018-0091-8  
1023 (2018).
- 1024 91 Corrigan, N. *et al.* Reversible-deactivation radical polymerization (controlled/living  
1025 radical polymerization): from discovery to materials design and applications. *Prog.*  
1026 *Polym. Sci.* **111**, doi:ARTN 10131110.1016/j.progpolymsci.2020.101311 (2020).
- 1027 92 Xu, J. T., Jung, K., Atme, A., Shanmugam, S. & Boyer, C. A robust and versatile  
1028 photoinduced living polymerization of conjugated and unconjugated monomers and its  
1029 oxygen tolerance. *J. Am. Chem. Soc.* **136**, 5508-5519, doi:10.1021/ja501745g (2014).
- 1030 93 Kottisch, V., Michaudel, Q. & Fors, B. P. Photocontrolled interconversion of cationic and  
1031 radical polymerizations. *J. Am. Chem. Soc.* **139**, 10665-10668, doi:10.1021/jacs.7b06661  
1032 (2017).

1033 94 Kracher, D. & Kourist, R. Recent developments in compartmentalization of  
1034 chemoenzymatic cascade reactions. *Curr. Opin. Green Sustainable Chem.* **32**, 100538,  
1035 doi:10.1016/j.cogsc.2021.100538 (2021).

1036 95 Chen, W.-H., Vázquez-González, M., Zoabi, A., Abu-Reziq, R. & Willner, I. Biocatalytic  
1037 cascades driven by enzymes encapsulated in metal-organic framework nanoparticles.  
1038 *Nat. Catal.* **1**, 689-695, doi:10.1038/s41929-018-0117-2 (2018).

1039 96 Quin, M. B., Wallin, K. K., Zhang, G. & Schmidt-Dannert, C. Spatial organization of multi-  
1040 enzyme biocatalytic cascades. *Org. Biomol. Chem.* **15**, 4260-4271,  
1041 doi:10.1039/c7ob00391a (2017).

1042 97 Wang, C., Yue, L. & Willner, I. Controlling biocatalytic cascades with enzyme-DNA  
1043 dynamic networks. *Nat. Catal.* **3**, 941-950, doi:10.1038/s41929-020-00524-7 (2020).

1044 98 Wilner, O. I. *et al.* Enzyme cascades activated on topologically programmed DNA  
1045 scaffolds. *Nat. Nanotechnol.* **4**, 249-254, doi:10.1038/nnano.2009.50 (2009).

1046 99 Zhang, Y. & Hess, H. Toward rational design of high-efficiency enzyme cascades. *ACS*  
1047 *Catal.* **7**, 6018-6027, doi:10.1021/acscatal.7b01766 (2017).

1048 100 Copéret, C. & Basset, J. M. Strategies to immobilize well-defined olefin metathesis  
1049 catalysts: supported homogeneous catalysis vs. surface organometallic chemistry. *Adv.*  
1050 *Synth. Catal.* **349**, 78-92, doi:10.1002/adsc.200600443 (2007).

1051 101 Gan, W., Dyson, P. J. & Laurency, G. Heterogeneous silica-supported ruthenium  
1052 phosphine catalysts for selective formic acid decomposition. *ChemCatChem* **5**, 3124-  
1053 3130, doi:10.1002/cctc.201300246 (2013).

1054 102 Wu, F., Feng, Y. & Jones, C. W. Recyclable silica-supported iridium bipyridine catalyst for  
1055 aromatic C-H borylation. *ACS Catal.* **4**, 1365-1375, doi:10.1021/cs4009539 (2014).

1056 103 Sévery, L. *et al.* Immobilization of molecular catalysts on electrode surfaces using host-  
1057 guest interactions. *Nat. Chem.*, doi:10.1038/s41557-021-00652-y (2021).

1058 104 Verho, O. & Backvall, J. E. Chemoenzymatic dynamic kinetic resolution: a powerful tool  
1059 for the preparation of enantiomerically pure alcohols and amines. *J. Am. Chem. Soc.*  
1060 **137**, 3996-4009, doi:10.1021/jacs.5b01031 (2015).

1061 105 Deiana, L. *et al.* Combined heterogeneous metal/chiral amine: multiple relay catalysis  
1062 for versatile eco-friendly synthesis. *Angew. Chem. Int. Ed.* **53**, 3447-3451,  
1063 doi:10.1002/anie.201310216 (2014).

1064 106 Palo-Nieto, C. *et al.* Integrated heterogeneous metal/enzymatic multiple relay catalysis  
1065 for eco-friendly and asymmetric synthesis. *ACS Catal.* **6**, 3932-3940,  
1066 doi:10.1021/acscatal.6b01031 (2016).

1067 107 Gustafson, K. P., Lihammar, R., Verho, O., Engstrom, K. & Backvall, J.-E. Chemoenzymatic  
1068 dynamic kinetic resolution of primary amines using a recyclable palladium nanoparticle  
1069 catalyst together with lipases. *J. Org. Chem.* **79**, 3747-3751, doi:10.1021/jo500508p  
1070 (2014).

1071 108 Wang, Y. *et al.* Electric-field-driven non-volatile multi-state switching of individual  
1072 skyrmions in a multiferroic heterostructure. *Nat. Commun.* **11**, 3577,  
1073 doi:10.1038/s41467-020-17354-7 (2020).

1074 109 Kodaimati, M. S., Gao, R., Root, S. E. & Whitesides, G. M. Magnetic fields enhance mass  
1075 transport during electrocatalytic reduction of CO<sub>2</sub>. *Chem. Catal* **2**, 797-815,  
1076 doi:10.1016/j.checat.2022.01.023 (2022).

1077 110 Aoyagi, S. *et al.* Control of chemical reaction involving dissolved oxygen using magnetic  
1078 field gradient. *Chem. Phys.* **331**, 137-141, doi:10.1016/j.chemphys.2006.10.006 (2006).  
1079 111 Kong, Y. *et al.* Mesoporous silica-supported rhodium complexes alongside organic  
1080 functional groups for catalysing the 1,4-addition reaction of arylboronic acid in water.  
1081 *Green Chem.* **24**, 3269-3276, doi:10.1039/D1GC04577F (2022).  
1082 112 Keim, W. Multiphase catalysis and its potential in catalytic processes: the story of  
1083 biphasic homogeneous catalysis. *Green Chem.* **5**, 105-111, doi:10.1039/B300138P  
1084 (2003).  
1085 113 Bényei, A. & Joó, F. Organometallic catalysis in aqueous solutions: the biphasic transfer  
1086 hydrogenation of aldehydes catalyzed by water-soluble phosphine complexes of  
1087 ruthenium, rhodium and iridium. *J. Mol. Catal.* **58**, 151-163, doi:10.1016/0304-  
1088 5102(90)85035-G (1990).  
1089 114 Cornils, B. & Kuntz, E. G. Introducing TPPTS and related ligands for industrial biphasic  
1090 processes. *J. Organomet. Chem.* **502**, 177-186, doi:10.1016/0022-328X(95)05820-F  
1091 (1995).  
1092 115 Alam, M. T. *et al.* The self-inhibitory nature of metabolic networks and its alleviation  
1093 through compartmentalization. *Nat. Commun.* **8**, 1-13, doi:10.1038/ncomms16018  
1094 (2017).  
1095 116 Avalos, J. L., Fink, G. R. & Stephanopoulos, G. Compartmentalization of metabolic  
1096 pathways in yeast mitochondria improves the production of branched-chain alcohols.  
1097 *Nat. Biotechnol.* **31**, 335-341, doi:10.1038/nbt.2509 (2013).  
1098 117 Jandt, U., You, C., Zhang, Y. H. P. & Zeng, A. P. Compartmentalization and metabolic  
1099 channeling for multienzymatic biosynthesis: practical strategies and modeling  
1100 approaches. *Adv. Biochem. Eng. Biotechnol.* **137**, 41-65, doi:10.1007/10\_2013\_221  
1101 (2013).  
1102 118 Tu, B. P. Logic of the yeast metabolic cycle: temporal compartmentalization of cellular  
1103 processes. *Science* **310**, 1152-1158, doi:10.1126/science.1120499 (2005).  
1104 119 Zecchin, A., Stapor, P. C., Goveia, J. & Carmeliet, P. Metabolic pathway  
1105 compartmentalization: an underappreciated opportunity? *Curr. Opin. Biotechnol.* **34**, 73-  
1106 81, doi:10.1016/j.copbio.2014.11.022 (2015).  
1107 120 Idan, O. & Hess, H. Origins of activity enhancement in enzyme cascades on scaffolds.  
1108 *ACS Nano* **7**, 8658-8665, doi:10.1021/nn402823k (2013).  
1109 121 Jordan, P. C. *et al.* Self-assembling biomolecular catalysts for hydrogen production. *Nat.*  
1110 *Chem.* **8**, 179-185, doi:10.1038/nchem.2416 (2016).  
1111 122 Simms, R. W. & Cunningham, M. F. Compartmentalization of reverse atom transfer  
1112 radical polymerization in miniemulsion. *Macromolecules* **41**, 5148-5155,  
1113 doi:10.1021/ma8003967 (2008).  
1114 123 Smeets, N. M. B., Heuts, J. P. A., Meuldijk, J., Cunningham, M. F. & Van Herk, A. M.  
1115 Evidence of compartmentalization in catalytic chain transfer mediated emulsion  
1116 polymerization of methyl methacrylate. *Macromolecules* **42**, 7332-7341,  
1117 doi:10.1021/ma9007829 (2009).  
1118 124 Thomson, M. E., Smeets, N. M. B., Heuts, J. P. A., Meuldijk, J. & Cunningham, M. F.  
1119 Catalytic chain transfer mediated emulsion polymerization: compartmentalization and

1120 its effects on the molecular weight distribution. *Macromolecules* **43**, 5647-5658,  
1121 doi:10.1021/ma100622b (2010).

1122 125 Pluth, M. D., Bergman, R. G. & Raymond, K. N. Acid catalysis in basic solution: a  
1123 supramolecular host promotes orthoformate hydrolysis. *Science* **316**, 85-88,  
1124 doi:10.1126/science.1138748 (2007).

1125 126 Pluth, M. D., Bergman, R. G. & Raymond, K. N. Supramolecular catalysis of orthoformate  
1126 hydrolysis in basic solution: An enzyme-like mechanism. *J. Am. Chem. Soc.* **130**, 11423-  
1127 11429, doi:10.1021/ja802839v (2008).

1128 127 Hart-Cooper, W. M., Clary, K. N., Toste, F. D., Bergman, R. G. & Raymond, K. N. Selective  
1129 monoterpene-like cyclization reactions achieved by water exclusion from reactive  
1130 intermediates in a supramolecular catalyst. *J. Am. Chem. Soc.* **134**, 17873-17876,  
1131 doi:10.1021/ja308254k (2012).

1132 128 Hong, C. M., Bergman, R. G., Raymond, K. N. & Toste, F. D. Self-assembled tetrahedral  
1133 hosts as supramolecular catalysts. *Acc. Chem. Res.* **51**, 2447-2455,  
1134 doi:10.1021/acs.accounts.8b00328 (2018).

1135 129 Morimoto, M. *et al.* Advances in supramolecular host-mediated reactivity. *Nat. Catal.* **3**,  
1136 969-984, doi:10.1038/s41929-020-00528-3 (2020).

1137 130 Dong, V. M., Fiedler, D., Carl, B., Bergman, R. G. & Raymond, K. N. Molecular recognition  
1138 and stabilization of iminium ions in water. *J. Am. Chem. Soc.* **128**, 14464-14465,  
1139 doi:10.1021/ja0657915 (2006).

1140 131 Kaphan, D. M., Toste, F. D., Bergman, R. G. & Raymond, K. N. Enabling new modes of  
1141 reactivity via constrictive binding in a supramolecular-assembly-catalyzed aza-prins  
1142 cyclization. *J. Am. Chem. Soc.* **137**, 9202-9205, doi:10.1021/jacs.5b01261 (2015).

1143 132 Davis, A., Liu, C. & Diaconescu, P. The art of compartment design for organometallic  
1144 catalysis. Preprint at <https://doi.org/10.26434/chemrxiv-22022-ng26434g26439> (2022).

1145 133 Pinson, J. & Podvorica, F. Attachment of organic layers to conductive or semiconductive  
1146 surfaces by reduction of diazonium salts. *Chem. Soc. Rev.* **34**, 429,  
1147 doi:10.1039/b406228k (2005).

1148 134 Engel, S., Fritz, E.-C. & Ravoo, B. J. New trends in the functionalization of metallic gold:  
1149 from organosulfur ligands to N-heterocyclic carbenes. *Chem. Soc. Rev.* **46**, 2057-2075,  
1150 doi:10.1039/c7cs00023e (2017).

1151 135 Jackson, M. N. & Surendranath, Y. Molecular control of heterogeneous electrocatalysis  
1152 through graphite conjugation. *Acc. Chem. Res.* **52**, 3432-3441,  
1153 doi:10.1021/acs.accounts.9b00439 (2019).

1154 136 Noda, H., Motokura, K., Miyaji, A. & Baba, T. Heterogeneous Synergistic Catalysis by a  
1155 Palladium Complex and an Amine on a Silica Surface for Acceleration of the Tsuji-Trost  
1156 Reaction. *Angew. Chem. Int. Ed.* **51**, 8017-8020, doi:10.1002/anie.201203066 (2012).

1157 137 Park, J.-W., Park, Y. J. & Jun, C.-H. Post-grafting of silica surfaces with pre-functionalized  
1158 organosilanes: new synthetic equivalents of conventional trialkoxysilanes. *Chem.*  
1159 *Commun.* **47**, 4860-4871, doi:10.1039/C1CC00038A (2011).

1160 138 Deiana, L. *et al.* Enantioselective heterogeneous synergistic catalysis for asymmetric  
1161 cascade transformations. *Adv. Synth. Catal.* **356**, 2485-2492 (2014).

1162 139 Deiana, L. *et al.* Artificial plant cell walls as multi-catalyst systems for enzymatic  
1163 cooperative asymmetric catalysis in non-aqueous media. *Chem. Commun.* **57**, 8814-  
1164 8817, doi:10.1039/D1CC02878B (2021).

1165 140 Engstrom, K. *et al.* Co-immobilization of an enzyme and a metal into the compartments  
1166 of mesoporous silica for cooperative tandem catalysis: an artificial metalloenzyme.  
1167 *Angew. Chem. Int. Ed.* **52**, 14006-14010, doi:10.1002/anie.201306487 (2013).

1168 141 Conley, M. P., Copéret, C. & Thieuleux, C. Mesostructured hybrid organic-silica  
1169 materials: ideal supports for well-defined heterogeneous organometallic catalysts. *ACS*  
1170 *Catal.* **4**, 1458-1469, doi:10.1021/cs500262t (2014).

1171 142 Materna, K. L., Crabtree, R. H. & Brudvig, G. W. Anchoring groups for photocatalytic  
1172 water oxidation on metal oxide surfaces. *Chem. Soc. Rev.* **46**, 6099-6110,  
1173 doi:10.1039/c7cs00314e (2017).

1174 143 Hanna, C. M., Luu, A. & Yang, J. Y. Proton-coupled electron transfer at anthraquinone  
1175 modified indium tin oxide electrodes. *ACS Appl. Energy Mater.* **2**, 59-65,  
1176 doi:10.1021/acsaem.8b01568 (2019).

1177 144 Bell, E. L. *et al.* Biocatalysis. *Nat. Rev. Methods Primers* **1**, doi:10.1038/s43586-021-  
1178 00044-z (2021).

1179 145 Bering, L., Thompson, J. & Micklefield, J. New reaction pathways by integrating chemo-  
1180 and biocatalysis. *Trends Chem.* **4**, 392-408, doi:10.1016/j.trechm.2022.02.008 (2022).

1181 146 Lauder, K. *et al.* Photo-biocatalytic one-pot cascades for the enantioselective synthesis  
1182 of 1,3-mercaptoalkanol volatile sulfur compounds. *Angew. Chem. Int. Ed.* **57**, 5803-5807,  
1183 doi:10.1002/anie.201802135 (2018).

1184 147 Betori, R. C., May, C. M. & Scheidt, K. A. Combined photoredox/enzymatic C-H benzylic  
1185 hydroxylations. *Angew. Chem. Int. Ed.* **58**, 16490-16494, doi:10.1002/anie.201909426  
1186 (2019).

1187 148 Sheldon, R. A. & van Pelt, S. Enzyme immobilisation in biocatalysis: why, what and how.  
1188 *Chem. Soc. Rev.* **42**, 6223-6235, doi:10.1039/c3cs60075k (2013).

1189 149 Talekar, S. *et al.* Parameters in preparation and characterization of cross linked enzyme  
1190 aggregates (CLEAs). *RSC Adv.* **3**, 12485-12511, doi:10.1039/c3ra40818c (2013).

1191 150 Sheldon, R. A. Characteristic features and biotechnological applications of cross-linked  
1192 enzyme aggregates (CLEAs). *Appl. Microbiol. Biotechnol.* **92**, 467-477,  
1193 doi:10.1007/s00253-011-3554-2 (2011).

1194 151 Cannon, G. C. *et al.* Microcompartments in prokaryotes: Carboxysomes and related  
1195 polyhedra. *Appl. Environ. Microbiol.* **67**, 5351-5361, doi:Doi 10.1128/Aem.67.12.5351-  
1196 5361.2001 (2001).

1197 152 Tanaka, S. *et al.* Atomic-level models of the bacterial carboxysome shell. *Science* **319**,  
1198 1083-1086, doi:10.1126/science.1151458 (2008).

1199 153 Vriezema, D. M. *et al.* Positional assembly of enzymes in polymersome nanoreactors for  
1200 cascade reactions. *Angewandte Chemie-International Edition* **46**, 7378-7382,  
1201 doi:10.1002/anie.200701125 (2007).

1202 154 Schmidt-Dannert, C. & Lopez-Gallego, F. A roadmap for biocatalysis - functional and  
1203 spatial orchestration of enzyme cascades. *Microbial Biotechnology* **9**, 601-609,  
1204 doi:10.1111/1751-7915.12386 (2016).

1205 155 Ouyang, Y., Zhang, P. & Willner, I. Dissipative biocatalytic cascades and gated transient  
1206 biocatalytic cascades driven by nucleic acid networks. *Science Advances* **8**,  
1207 doi:10.1126/sciadv.abn3534 (2022).

1208 156 Heuson, E. *et al.* Optimisation of catalysts coupling in multi-catalytic hybrid materials:  
1209 perspectives for the next revolution in catalysis. *Green Chem.* **23**, 1942-1954,  
1210 doi:10.1039/d0gc04172f (2021).

1211 157 Dickie, R. A., Labana, S. S. & Bauer, R. S. in *Cross-linked polymers: Chemistry, properties,*  
1212 *and applications.* (American Chemical Society, Washington, DC, 1988).

1213 158 Maitra, J. & Shukla, V. K. Cross-linking in hydrogels-a review. *Am. J. Polym. Sci* **4**, 25-31,  
1214 doi:10.5923/j.ajps.20140402.01 (2014).

1215 159 Delle Chiaie, K. R. *et al.* Redox-triggered crosslinking of a degradable polymer. *Polym.*  
1216 *Chem.* **7**, 4675-4681, doi:10.1039/c6py00975a (2016).

1217 160 Jia, X., Qin, C., Friedberger, T., Guan, Z. & Huang, Z. Efficient and selective degradation of  
1218 polyethylenes into liquid fuels and waxes under mild conditions. *Sci. Adv.* **2**, e1501591,  
1219 doi:10.1126/sciadv.1501591 (2016).

1220 161 Haibach, M. C., Kundu, S., Brookhart, M. & Goldman, A. S. Alkane metathesis by tandem  
1221 alkane-dehydrogenation-olefin-metathesis catalysis and related chemistry. *Acc. Chem.*  
1222 *Res.* **45**, 947-958, doi:10.1021/ar3000713 (2012).

1223 162 Coperet, C., Liao, W. C., Gordon, C. P. & Ong, T. C. Active sites in supported single-site  
1224 catalysts: an NMR perspective. *J. Am. Chem. Soc.* **139**, 10588-10596,  
1225 doi:10.1021/jacs.6b12981 (2017).

1226 163 Weisz, P. B. & Hicks, J. S. The behaviour of porous catalyst particles in view of internal  
1227 mass and heat diffusion effects. *Chem. Eng. Sci.* **17**, 265-275, doi:Doi 10.1016/0009-  
1228 2509(62)85005-2 (1962).

1229 164 Weisz, P. B. Diffusion and chemical transformation: an interdisciplinary excursion.  
1230 *Science* **179**, 433-440, doi:10.1126/science.179.4072.433 (1973).

1231 165 Rayder, T. M., Adillon, E. H., Byers, J. A. & Tsung, C.-K. A bioinspired multicomponent  
1232 catalytic system for converting carbon dioxide into methanol autocatalytically. *Chem* **6**,  
1233 1742-1754, doi:10.1016/j.chempr.2020.04.008 (2020).

1234 166 Wayland, B. B., Ba, S. & Sherry, A. E. Activation of methane and toluene by rhodium(II)  
1235 porphyrin complexes. *J. Am. Chem. Soc.* **113**, 5305-5311, doi:10.1021/ja00014a025  
1236 (1991).

1237 167 Nielsen, D. U., Hu, X.-M., Daasbjerg, K. & Skrydstrup, T. Chemically and  
1238 electrochemically catalysed conversion of CO<sub>2</sub> to CO with follow-up utilization to value-  
1239 added chemicals. *Nat. Catal.* **1**, 244-254, doi:10.1038/s41929-018-0051-3 (2018).

1240 168 Dodge, H. *et al.* Polyketones from Carbon Dioxide and Ethylene by Integrating  
1241 Electrochemical and Organometallic Catalysis. Preprint at  
1242 <https://doi.org/10.26434/chemrxiv-22022-c26439gkl> (2022).

1243 169 Chen, T. T., Zhu, Y. & Williams, C. K. Pentablock copolymer from tetracomponent  
1244 monomer mixture using a switchable dizinc catalyst. *Macromolecules* **51**, 5346-5351,  
1245 doi:10.1021/acs.macromol.8b01224 (2018).

1246 170 Lewandowski, B. *et al.* Sequence-specific peptide synthesis by an artificial small-  
1247 molecule machine. *Science* **339**, 189-193, doi:10.1126/science.1229753 (2013).

1248 171 Qi, M. *et al.* Electrochemically switchable polymerization from surface-anchored  
1249 molecular catalysts. *Chem. Sci.* **12**, 9042-9052, doi:10.1039/d1sc02163j (2021).

1250 172 Steiner, S. *et al.* Organic synthesis in a modular robotic system driven by a chemical  
1251 programming language. *Science* **363**, 144-144, doi:10.1126/science.aav2211 (2019).

1252 173 Baker, M. 1,500 scientists lift the lid on reproducibility. *Nature* **533**, 452-454 (2016).

1253 174 Diebolt, O., van Leeuwen, P. W. N. M. & Kamer, P. C. J. Operando Spectroscopy in  
1254 Catalytic Carbonylation Reactions. *ACS Catal.* **2**, 2357-2370, doi:10.1021/cs300471s  
1255 (2012).

1256 175 Köhnke, K. *et al.* Operando monitoring of mechanisms and deactivation of molecular  
1257 catalysts. *Green Chem.* **24**, 1951-1972, doi:10.1039/D1GC04383H (2022).

1258 176 Webb, D. & Jamison, T. F. Continuous flow multi-step organic synthesis. *Chem. Sci.* **1**,  
1259 675, doi:10.1039/c0sc00381f (2010).

1260 177 Noël, T., Cao, Y. & Laudadio, G. The Fundamentals Behind the Use of Flow Reactors in  
1261 Electrochemistry. *Acc. Chem. Res.* **52**, 2858-2869, doi:10.1021/acs.accounts.9b00412  
1262 (2019).

1263 178 Pletcher, D., Green, R. A. & Brown, R. C. D. Flow electrolysis cells for the synthetic  
1264 organic chemistry laboratory. *Chem. Rev.* **118**, 4573-4591,  
1265 doi:10.1021/acs.chemrev.7b00360 (2018).

1266 179 Britton, J. & Jamison, T. F. The assembly and use of continuous flow systems for  
1267 chemical synthesis. *Nat. Protoc.* **12**, 2423-2446, doi:10.1038/nprot.2017.102 (2017).

1268 180 Bannock, J. H., Krishnadasan, S. H., Heeney, M. & de Mello, J. C. A gentle introduction to  
1269 the noble art of flow chemistry. *Mater. Horiz.* **1**, 373-378, doi:10.1039/C4MH00054D  
1270 (2014).

1271 181 Hartman, R. L., McMullen, J. P. & Jensen, K. F. Deciding whether to go with the flow:  
1272 evaluating the merits of flow reactors for synthesis. *Angew. Chem. Int. Ed.* **50**, 7502-  
1273 7519, doi:10.1002/anie.201004637 (2011).

1274 182 Jia, Z. J., Shan, G., Daniliuc, C. G., Antonchick, A. P. & Waldmann, H. Enantioselective  
1275 synthesis of the spirotropanyl oxindole scaffold through bimetallic relay catalysis.  
1276 *Angew. Chem. Int. Ed.* **57**, 14493-14497, doi:10.1002/anie.201712882 (2018).

1277 183 Dhiman, S., Mishra, U. K. & Ramasastry, S. S. V. One-pot trimetallic relay catalysis: a  
1278 unified approach for the synthesis of beta-carbolines and other [c]-fused pyridines.  
1279 *Angew. Chem. Int. Ed.* **55**, 7737-7741, doi:10.1002/anie.201600840 (2016).

1280 184 Yu, Q. L. *et al.* Enantioselective oxidative phenol-indole [3+2] coupling enabled by  
1281 biomimetic Mn(III)/Bronsted acid relay catalysis. *ACS Catal.* **9**, 7285-7291,  
1282 doi:10.1021/acscatal.9b01734 (2019).

1283 185 Atesin, A. C., Ray, N. A., Stair, P. C. & Marks, T. J. Etheric C-O bond hydrogenolysis using  
1284 a tandem lanthanide triflate/supported palladium nanoparticle catalyst system. *J. Am.*  
1285 *Chem. Soc.* **134**, 14682-14685, doi:10.1021/ja306309u (2012).

1286 186 Lohr, T. L., Li, Z. & Marks, T. J. Thermodynamic strategies for C-O bond formation and  
1287 cleavage via tandem catalysis. *Acc. Chem. Res.* **49**, 824-834,  
1288 doi:10.1021/acs.accounts.6b00069 (2016).

1289 187 Martinez, S., Veth, L., Lainer, B. & Dydio, P. Challenges and opportunities in  
1290 multicatalysis. *ACS Catal.* **11**, 3891-3915, doi:10.1021/acscatal.0c05725 (2021).

1291 188 Gromski, P. S., Granda, J. M. & Cronin, L. Universal chemical synthesis and discovery  
1292 with 'the chemputer'. *Trends Chem.* **2**, 4-12, doi:10.1016/j.trechm.2019.07.004 (2020).  
1293

## 1294 **Acknowledgements**

1295 We thank the National Science Foundation as part of the Center for Integrated Catalysis (CHE-  
1296 2023955) for supporting this work. Shijie Deng is grateful for an INFEWS fellowship (NSF Grant  
1297 DGE-1735325).

## 1298 **Competing interests**

1299 The authors declare no competing interests.

## 1300 **Related links**

1301 PolyInfo: <https://polymer.nims.go.jp/en/>

1302 Polymer Property Predictor and Database: [https://www.nist.gov/programs-projects/polymer-property-](https://www.nist.gov/programs-projects/polymer-property-predictor-and-database)  
1303 [predictor-and-database](https://www.nist.gov/programs-projects/polymer-property-predictor-and-database)

1304 CAMPUS: <https://www.campusplastics.com>

1305

## 1306 **Highlighted**

## **references**

1307 1. Rayder, T. M., Bensalah, A. T., Li, B., Byers, J. A. & Tsung, C.-K. Engineering second sphere  
1308 interactions in a host-guest multicomponent catalyst system for the hydrogenation of carbon  
1309 dioxide to methanol. *J. Am. Chem. Soc.* **143**, 1630-1640, doi:10.1021/jacs.0c08957 (2021)

1310 **Summary: This paper describes the encapsulation of two different Ru catalysts alongside**  
1311 **second-sphere amines in MOFs to enable efficient carbon dioxide hydrogenation to**  
1312 **methanol.**

1313

1314 2. Natinsky, B. S., Lu, S., Copeland, E. D., Quintana, J. C. & Liu, C. Solution catalytic cycle of  
1315 incompatible steps for ambient air oxidation of methane to methanol. *ACS Cent. Sci.* **5**, 1584-  
1316 1590, doi:10.1021/acscentsci.9b00625 (2019).

1317 **Summary: This paper describes reconciling incompatible rhodium-catalyzed C-H**  
1318 **activation of methane with air-mediated methanol formation via the employment of an**  
1319 **oxygen gradient generated by a nanowire array electrode.**

1320

1321 3. Jolly, B. J., Co, N. H., Davis, A. R., Diaconescu, P. L. & Liu, C. A generalized kinetic model for  
1322 compartmentalization of organometallic catalysis. *Chem. Sci.* **13**, 1101-1110,  
1323 doi:10.1039/D1SC04983F (2022)

1324 **Summary: This paper presents a theoretical framework and design principles for**  
1325 **designing spatial confinement for a catalytic cycle with careful control of diffusivity in and**  
1326 **out of the compartment.**

1327

1328 4. Lorkovic, I. M., Duff, R. R. & Wrighton, M. S. Use of the redox-active ligand 1, 1'-bis  
1329 (diphenylphosphino) cobaltocene to reversibly alter the rate of the rhodium (I)-catalyzed reduction

1330 and isomerization of ketones and alkenes. *J. Am. Chem. Soc.* **117**, 3617-3618,  
1331 doi:10.1021/ja00117a033 (1995).

1332 **Summary: This paper is the first example demonstrating redox switchable catalysis.**

1333

1334 5. Qi, M., Dong, Q., Wang, D. & Byers, J. A. Electrochemically Switchable Ring-Opening  
1335 Polymerization of Lactide and Cyclohexene Oxide. *J. Am. Chem. Soc.* **140**, 5686-5690,  
1336 doi:10.1021/jacs.8b02171 (2018)

1337 **Summary: This paper describes an electrochemical setup for redox switchable**  
1338 **polymerization.**

1339

1340 6. Quan, S. M., Wang, X., Zhang, R. & Diaconescu, P. L. Redox switchable copolymerization of  
1341 cyclic esters and epoxides by a zirconium complex. *Macromolecules* **49**, 6768-6778,  
1342 doi:10.1021/acs.macromol.6b00997 (2016).

1343 **Summary: This paper reports the first example of synthesizing tri- and tetrablock**  
1344 **copolymers by using redox switchable copolymerization.**

1345

1346 7. Yoon, H. J., Kuwabara, J., Kim, J. H. & Mirkin, C. A. Allosteric supramolecular triple-layer  
1347 catalysts. *Science* **330**, 66-69, doi:10.1126/science.1193928 (2010).

1348 **Summary: This paper describes using chloride anion as a chemical switch for ring opening**  
1349 **polymerization.**

1350

1351 8. Kita, M. R. & Miller, A. J. M. Cation-modulated reactivity of iridium hydride pincer-crown ether  
1352 complexes. *J. Am. Chem. Soc.* **136**, 14519-14529, doi:10.1021/ja507324s (2014).

1353 **Summary: This paper describes how cations can be used to tune the reaction rate for**  
1354 **hydrogen activation.**

1355

1356 9. Cai, Z. Z., Xiao, D. W. & Do, L. H. Fine-tuning nickel phenoxyimine olefin polymerization  
1357 catalysts: performance boosting by alkali cations. *J. Am. Chem. Soc.* **137**, 15501-15510,  
1358 doi:10.1021/jacs.5b10351 (2015).

1359 **Summary: This paper describes how alkali cations can be used to regulate the reaction**  
1360 **rate for ethylene polymerization and the structure of the resulting polymer.**

1361

1362 10. Romain, C. & Williams, C. K. Chemoselective polymerization control: from mixed-monomer  
1363 feedstock to copolymers. *Angew. Chem. Int. Ed.* **53**, 1607-1610, doi:10.1002/anie.201309575  
1364 (2014).

1365 **Summary: This paper presents an example of using CO<sub>2</sub> to shuttle a catalyst between two**  
1366 **different polymerization cycles.**

1367

1368 11. Eisenreich, F. *et al.* A photoswitchable catalyst system for remote-controlled  
1369 (co)polymerization in situ. *Nat. Catal.* **1**, 516-522, doi:10.1038/s41929-018-0091-8 (2018).

1370 **Summary: This paper demonstrates how light-programmed copolymer synthesis can be**  
1371 **achieved using a photoswitchable catalyst.**

1372

1373 12. Chen, W.-H., Vázquez-González, M., Zoabi, A., Abu-Reziq, R. & Willner, I. Biocatalytic  
1374 cascades driven by enzymes encapsulated in metal-organic framework nanoparticles. *Nat. Catal.*  
1375 **1**, 689-695, doi:10.1038/s41929-018-0117-2 (2018).

1376 **Summary: This article presents the spatial confinement of two to three enzyme cascades**  
1377 **within ZIF-8 MOFs for improved intermediate channeling between active sites.**

1378  
1379 13. Lu, J., Dimroth, J. & Weck, M. Compartmentalization of incompatible catalytic transformations  
1380 for tandem catalysis. *J. Am. Chem. Soc.* **137**, 12984-12989, doi:10.1021/jacs.5b07257 (2015).

1381 **Summary: This paper demonstrates the preparation of a polymer micelle to encapsulate**  
1382 **two catalysts in close proximity and use them to carry out an incompatible tandem reaction**  
1383 **sequence.**

1384  
1385 14. Copéret, C. & Basset, J. M. Strategies to immobilize well-defined olefin metathesis catalysts:  
1386 supported homogeneous catalysis vs. surface organometallic chemistry. *Adv. Synth. Catal.* **349**,  
1387 78-92 (2007).

1388 **Summary: This review (and the cited articles within) describes various methods to**  
1389 **immobilize olefin metathesis catalysts onto solid supports.**

1390  
1391 15. Pluth, M. D., Bergman, R. G. & Raymond, K. N. Acid catalysis in basic solution: a  
1392 supramolecular host promotes orthoformate hydrolysis. *Science* **316**, 85-88 (2007).

1393 **Summary: This article describes synthetic host-guest systems that mimic electrostatic**  
1394 **encapsulation of enzyme pockets to enable acid-catalyzed reactions in a basic**  
1395 **environment.**

1396  
1397 16. Engstrom, K. *et al.* Co-immobilization of an Enzyme and a Metal into the Compartments of  
1398 Mesoporous Silica for Cooperative Tandem Catalysis: An Artificial Metalloenzyme. *Angew. Chem.*  
1399 *Int. Ed.* **52**, 14006-14010, doi:10.1002/anie.201306487 (2013).

1400 **Summary: This paper presents the co-encapsulation of Pd nanoparticles and an enzyme**  
1401 **within amine/imine functionalized silica for synergistic primary amine kinetic resolution.**

1402  
1403 17. Wang, Chen, Liang Yue, and Itamar Willner. "Controlling biocatalytic cascades with enzyme-  
1404 DNA dynamic networks." *Nat. Catal.* **3**, 941-950 (2020).

1405 **Summary: This paper describes nucleic acid-enzyme conjugate networks to design**  
1406 **triggered biocatalytic cascades to construct controlled (switchable) biocatalytic networks.**

1407  
1408 18. Jia, X., Qin, C., Friedberger, T., Guan, Z. & Huang, Z. Efficient and selective degradation of  
1409 polyethylenes into liquid fuels and waxes under mild conditions. *Sci. Adv.* **2**, e1501591,  
1410 doi:10.1126/sciadv.1501591 (2016).

1411 **Summary: This paper presents how spatially separating an alkane**  
1412 **dehydrogenation/hydrogenation catalyst and an alkene metathesis catalyst can**  
1413 **circumvent unwanted catalyst-catalyst interactions.**

1414  
1415 19. Lewandowski, B. *et al.* Sequence-specific peptide synthesis by an artificial small-molecule  
1416 machine. *Science* **339**, 189-193 (2013).

1417 **Summary: This paper demonstrates how artificial templating can mimic sequence-defined**  
1418 **peptide synthesis.**

1419  
1420 20. Qi, M. *et al.* Electrochemically switchable polymerization from surface-anchored molecular  
1421 catalysts. *Chem. Sci.* **12**, 9042-9052, doi:10.1039/d1sc02163j (2021).

1422 **Summary: This paper details the immobilization of Fe(II) and Fe(III) bis-iminopyridine**  
1423 **catalysts onto an electrochemically active surface to generate patterned polylactide and**  
1424 **poly(cyclohexene oxide) surfaces via switchable ring opening polymerization.**

1425  
1426 21. Steiner, S. *et al.* Organic synthesis in a modular robotic system driven by a chemical  
1427 programming language. *Science* **363**, eaav2211 (2019).

1428 **Summary: This paper demonstrates how programming and automation can be integrated**  
1429 **into laboratory chemical synthesis to improve efficiency.**

1430